5-2016

The Apoptotic and Inhibitory Effects of Phylloquinone in the U937 Cell Line

Tesha E. Blair
East Tennessee State Universtiy

The Apoptotic and Inhibitory Effects of Phylloquinone in the U937 Cell Line

---

A thesis

presented to

the faculty of the Department of Biological Sciences

East Tennessee State University

In partial fulfillment

of the requirements for the degree

Master of Science in Biology

---

by

Tesha Blair

May 2016

Hugh Miller III, Ph.D., Chair

Aruna Kilaru, Ph.D.

Leonard Robertson, Ph.D.

Keywords: apoptosis, phylloquinone, vitamin K, cell death, U937 cells

ABSTRACT

The Apoptotic and Inhibitory Effects of Phylloquinone in the U937 Cell Line

by

Tesha Blair

Phylloquinone is a natural analog of vitamin K that has been shown to both inhibit cancer cell growth and induce apoptosis in several cancer cell lines. This study examined these effects in a non-Hodgkin lymphoma cell line, known as U937. Cell growth inhibition and apoptosis were assessed through the quantification of cell density and area, following treatment with several concentrations of phylloquinone. In addition, apoptosis was detected and quantified using immunofluorescent markers of apoptosis (i.e. annexin V, APO-BrdU). Treatment with phylloquinone resulted in reduced overall cell density, increased overall cell area, and an increased frequency of apoptosis in U937 cells. Increasing both phylloquinone concentration and treatment time enhanced these effects. These results are significant because they document the anti-cancer effects of this analog of vitamin K, as well as provide insight into the morphological changes that occur during apoptosis in U937 cells.

ACKNOWLEDGEMENTS

I would like to thank my mentor and advisor Dr. Hugh Miller for his support and guidance throughout my time in graduate school at East Tennessee State University. I would also like to thank my committee members Dr. Aruna Kilaru and Dr. Leonard Robertson for their advisement and input on my thesis project. I would also like to thank Dr. Thomas Jones and Dr. Lev Yampolsky, as well as fellow graduate student Adam McCullough.

Special thanks go out to my mom and dad, as well as the rest of my family and friends for supporting and encouraging me in everything I do.

TABLE OF CONTENTS

Page

LIST OF TABLES

Table Page

LIST OF FIGURES

Figure Page

CHAPTER 1

INTRODUCTION

The National Institute of Health estimates the allocation of $9.3 billion dollars to fund cancer-related research for the year of 2017 (National Institute of Health 2016). This comes as no surprise, considering the millions of cancer fatalities worldwide every year. Risk factors like nutritional deficiencies, environmental toxins, transmission of disease, and an ever-growing and aging population directly contribute to the rising number of new cancer cases (Peterson et al. 2012; Howell et al. 2014; American Cancer Society 2015). The World Health Organization predicts that by 2035, the worldwide rates of cancer morbidity and mortality will reach 24 million and 14.6 million, respectively (National Cancer Institute 2015). In order to combat this epidemic, more effective and accessible treatments need to be developed. Many researchers are currently interested in the relationship between cell proliferation and cell death – specifically, the dysregulation of genetically directed cell death pathways, like apoptosis, in the proliferation of aberrant cells, and how this relationship can be used to design more promising cancer treatment therapies (Lowe and Lin 2000).

Apoptosis

The earliest documentation of cell death dates back to 1842, when a German scientist named Carl Vogt published a study on the degeneration of cells during metamorphosis of the common midwife toad (*Alytes obstetricans*) (Clarke and

Clarke 2012). A little over forty years later, another German scientist named Walter Flemming characterized the morphological changes of non-necrotic cell death in his publication on ovarian follicular cell atresia, which is a normal process of menstruation (Lockshin and Zakeri 2001). It was not until 1972 that the term "apoptosis" was first proposed by pathologists John Foxton Ross Kerr, Andrew H. Wyllie, and Alastair Robert Currie, to describe a type of cell death morphologically separate from necrosis, as well as one that is fundamental to the homeostatic balance between cell division and cell death in normal animal cell populations (Kerr et al. 1972; Bold et al. 1997; Jiang 2011). Since the recognition that apoptosis is a genetically regulated event that occurs both during normal development and aging, and in response to various internal and external stimuli, many scientists have been interested in the factors affecting this type of cell death, as well as the biochemical and molecular pathways coordinating their effect (Williams and Smith 1993; Elmore 2007).

Kerr, Wyllie, and Currie derived the term "apoptosis" from the Greek word "αποπτωσισ", which translates to the "dropping off" or "falling off" of flower petals or tree leaves, to describe the structural changes they observed in a variety of tissues with electron microscopy, including neonatal rat adrenal cortexes and human neoplasms (Kerr et al. 1972). This derivation was likely selected because it implies that the death or loss of a specific part of an organism is fundamental to the continuation of its life cycle. Prior to this time, the morphology of cell death described in most scientific texts was characteristic of coagulative or classical necrosis, and therefore apoptosis was seen as a distinct subtype of necrosis, known

as “shrinkage necrosis”, with markedly different morphological changes (Kerr 1971; Kerr 2002). The process of apoptosis, as first described by Kerr, Wyllie, and Currie in 1972, generally affects individual cells scattered throughout cell populations, and occurs in two discrete stages. The first stage consists of the formation of apoptotic bodies, which are preserved cellular fragments containing organelles, condensed cytoplasm, and/or condensed nuclear chromatin, which are chemically and structurally intact. The second stage of apoptosis consists of the phagocytosis and subsequent degradation of apoptotic bodies by nearby cells (Kerr et al. 1972; Kerr et al. 1994).

Morphology

The formation of apoptotic bodies occurs through a series of coordinated events. The apoptotic cell undergoes simultaneous nuclear shrinkage or pyknosis, membrane blebbing or the appearance of protrusions along the cell’s surface, and cytoplasmic condensation (Kerr et al. 1972). This is followed by nuclear fragmentation or karyorrhexis, and finally, the separation of protuberances along the cell’s surface to form membrane-bound apoptotic bodies (Kerr et al. 1972; Majno and Joris 1995). The term “budding” has also been used to refer to the formation of apoptotic cell bodies (Kerr et al. 1994; Majno and Joris 1995). Apoptotic bodies can contain any cellular components that were near or in the cytoplasmic protrusion before budding occurred, including cytoplasmic elements, condensed organelles, and condensed nuclear chromatin. Although size and

composition is highly variable between bodies, the structural and chemical integrity of their contents is preserved (Kerr et al. 1972; Kerr et al. 1994).

Following the release of chemoattractants and surface signals, apoptotic bodies are rapidly phagocytized by a variety of adjacent cell types, including macrophages, neoplastic cells, epithelial cells, or fibroblasts, and undergo lysosomal degradation (Kerr et al. 1972; Majno and Joris 1995; Elmore 2007; Elliot and Ravichandran 2010). A renowned feature of apoptosis is that, unlike necrosis, no inflammation results from the displacement of cellular bodies (Kerr et al. 1994; Majno and Joris 1995). There are several reasons why apoptosis does not provoke an inflammatory response: (1) apoptotic bodies are membrane-bound, so cellular contents are not spilled into interstitial tissues surrounding the cell, (2) bodies are quickly engulfed by nearby cells, inhibiting secondary necrosis, and (3) anti-inflammatory cytokines are not produced by phagocytic cells (Martin and Green 1995; Elmore 2007; Silva 2010). Due to this lack of inflammation, apoptosis represents a promising way to ensure specific cell death without damage to surrounding healthy tissues.

Programmed Cell Death and Cell Suicide – Incidence of Apoptosis

Programmed cell death (PCD) and cell suicide are both terms used to describe apoptosis, although they have alternate connotations. PCD denotes cell death that is genetically predetermined, while cell suicide implies an inducible or spontaneous form of cell death. The pervasiveness of these expressions has led to some ambiguity in regards to the circumstances surrounding apoptosis (Majno and

Joris 1995). In truth, apoptosis can be predetermined or inducible depending on the life stage of the organism and its environment. This type of cell death has two major roles – one is to ensure the existence of healthy cells, the other is to diminish the existence of unhealthy ones (Kerr et al. 1994). In this way, PCD can generally be applied to the role of apoptosis in healthy cell populations, while cell suicide can be used to depict the role of apoptosis in unhealthy ones.

Apoptosis ensures the proliferation of healthy cells through the regulated deletion of cells that are overabundant, or cells that have lost their function or become superfluous over time (Kerr et al. 1972; Martin and Green 1995). During ontogenesis, and particularly throughout embryogenesis, the controlled deletion of overabundant cells is necessary for shaping an organism's developing tissues and organs (Martin and Green 1995; Abud 2004). A renowned example of apoptosis during embryogenesis occurs in primates, where one of its many responsibilities is the elimination of the interdigital webbing of the hand or foot to form fingers and toes (Dorn 2013). Apoptosis is also critical to the excision of cells that are no longer needed or have lost their function during events like metamorphosis and aging (Martin and Green 1995). During amphibian metamorphosis, for example, this type of cell death is responsible for the removal of the tadpole's tail as it matures into an adult frog (Kerr et al. 1974). These events provide examples of apoptosis that are genetically programmed or predetermined, and are essential to the growth or maintenance of healthy cell populations.

Apoptosis diminishes the existence of unhealthy or abnormal cells in response to a number of factors, including mutation and disease (Martin and Green

1995; Elmore 2007). It goes without saying that the accumulation of aberrant cells compromises the body's ability to defend itself. Therefore, in individuals with normal physiology, the induction of apoptosis is one of first lines of defense in or against cells that are structurally and functionally damaged (Kerr et al. 1994). Without this inducible form of cell death, cell populations would accumulate more mutations and be more susceptible to a variety of diseases. For instance, there is a strong correlation between modified apoptotic pathways resulting in less cell death and an increased incidence of cancer (Kerr et al. 1994; Bold et al. 1997). Other examples of the relationship between reduced apoptosis and enhanced morbidity include increased susceptibility to viral infection, like Epstein-Barr and adenovirus, as well as to autoimmune disease, like lupus and rheumatoid arthritis (Solary et al. 1996). Typically, the ability to engage in cell suicide is beneficial to the specific cell population, and therefore, many pathologic states arise from an inability to engage in this form of cell death. There are instances, however, when modifications causing the upregulation of this cell death pathway can accelerate the progression of a disorder or disease (Elmore 2007). This is exemplified by viruses that can induce apoptosis to aid in their own propagation, by either causing an infected cell to die and release its viral constituents (e.g. Avian Reovirus) or causing the death of an immune cell, so that it is unable to phagocytize the virus (e.g. HIV and influenza A and B viruses) (Hinshaw et al. 1994; Elmore 2007; Rodríguez-Grille et al. 2014). These examples provide evidence of the role of this inducible form of cell death in diminishing the existence of unhealthy cells, as well as the some of the consequences of modulations to these pathways.

Biochemical Mechanisms

The mechanisms of apoptosis can be divided into two major pathways: the extrinsic or death receptor pathway and the intrinsic or mitochondrial pathway (Elmore 2007). Both pathways are mediated by caspases, a group of cysteine proteases, which remain in their zymogenic form until they receive an apoptotic stimulus (Johnstone et al. 2002). Once active, caspases engage in a caspase cascade where upstream or initiator caspases (e.g. caspases 2, 8, 9, 10) cleave downstream or effector caspases (e.g. caspases 3, 6, 7), which, in turn, cleave various cellular proteins that regulate apoptotic cell death (Chang and Yang 2000; Turk and Stoka 2007). The extrinsic pathway of apoptosis is initiated when an extrinsic ligand binds to a membrane-bound member of the tumor necrosis factor (TNF) receptor superfamily (e.g. TRAIL receptor 1, Fas receptor), which is commonly referred to as a "death receptor" (Johnstone et al. 2002; Wang and El-Deiry 2003). Binding of these receptors results in the activation of initiator caspases 8 and 10, which activate effector caspases 3 and 7 (Johnstone et al. 2002). These caspases then activate a network of proteins and orchestrate numerous processes that lead to apoptotic cell death (Chang and Yang 2000; Elmore 2007).

The intrinsic pathway of apoptosis is initiated when the cell is exposed to DNA damage, free radicals, radiation, viral infections, and other types of cell stress (Wang and El-Deiry 2003). These stimuli activate pro-apoptotic members of the Bcl-2 superfamily (e.g. PUMA, Bax, Bak), which modify the integrity of the inner mitochondrial membrane and result in the release of several pro-apoptotic proteins (e.g. cytochrome c, Smac, Omi) into the cytosol (Johnstone et al. 2002; Turk and

Stoka 2007). Cytochrome c activates apaf1, which is needed for the formation of an apoptosome, a quaternary protein structure containing cytochrome c and apaf1, and the activation of initiator caspase 9 (Johnstone et al. 2002; Turk and Stoka 2007). The activation of caspase 9 triggers a caspase cascade and activates effector caspases 3, 6, and 7, whilst Smac and Omi bind to and antagonize several anti-apoptotic proteins (Johnstone et al. 2002). Again, this cascade ultimately leads to activation and induction of a variety of proteins and processes that lead to apoptotic cell death (Chang and Yang 2000; Elmore 2007). There is evidence of crosstalk between the pathways: caspase 8 can activate another Bcl-2 family member, Bid, which can induce the release of cytochrome c in the mitochondria through interaction with Bax and Bak (Johnstone et al. 2002; Wang and El-Deiry 2003).

A third apoptotic pathway does exist, but it is limited to natural killer cells and cytotoxic T cells. These cells secrete a serine protease called granzyme B, which is similar to caspases because they both cleave other proteins directly following an aspartic acid residue (Turk and Stoka 2007). When natural killer cells or cytotoxic T cells encounter a target cell, they can secrete granzyme B, along with perforin, and engage in the extrinsic pathway through cleavage of caspase 3 or in the intrinsic pathway through cleavage of Bid (Turk and Stoka 2007). Another serine protease, granzyme A, is secreted by cytotoxic T cells and can induce apoptosis through a caspase independent pathway involving tumor suppressor gene, NM23-H1 (Elmore 2007). Granzyme A cleaves NM23-H1 antagonist SET, which activates NM23-H1 and results in apoptotic DNA degradation (Elmore 2007).

Apoptosis and Cancer

Apoptosis is fundamental to the homeostasis of healthy cell populations – that is, the balance between cell growth and division, as well as cell death. Any disruption to this balance will therefore result in numerous pathologic states, including cancer (Kerr et al. 1972; Alberts et al. 2002). Cancer is the result of defects or modifications to genes controlling cell proliferation and differentiation, as well as those controlling cell death (Martin and Green 1995). With regards to cell death, specifically apoptosis, there are two major categories of genes: repressors or anti-apoptotic genes and inducers or pro-apoptotic genes. As their names suggest, repressors inhibit or postpone apoptosis, while inducers provoke it or increase the likelihood that it will occur (Martin and Green 1995). Mutations or modifications to the expression levels of repressors and/or inducers in both apoptotic pathways, as well as their upstream and downstream components, are common to many cancer and tumor types, although these changes more often occur in members of the intrinsic or mitochondrial pathway (Martin and Green 1995; Johnstone et al. 2002).

The p53 tumor suppressor gene is a checkpoint protein that is essential to the regulation of both the cell cycle and cell death (Kerr et al. 1994; Bold et al. 1997; Lowe and Lin 2000). p53 allows cells to respond to DNA damage by arresting the cell cycle and attempting DNA repair, when its levels are low or moderate, and inducing apoptosis when its levels are high (Bold et al. 1997). The wild-type p53 allele is an intrinsic inducer of apoptosis and is responsible for the transcriptional activation of Bcl-2 family inducers (e.g. Bax, Bak, PUMA) and repression of Bcl-2 family suppressors (e.g. Bcl-2, Bcl-X) (Johnstone et al. 2002). The loss of function

that occurs in mutant p53 alleles has been found to both inactivate apoptosis and accelerate tumor formation, and has been observed in the vast majority of human cancer types, including lung, colon, breast, prostate, and pancreas, (Bold et al. 1997; Lowe and Lin 2000; Johnstone et al. 2002). For this reason, functional mutations of p53 are associated with advanced stage cancer and high mortality (Lowe and Lin 2000). In addition to changes in p53 itself, mutations or modified expression of its upstream regulators (e.g. ATM, Mdm 2) or downstream effectors (e.g. Bax, Bak, Apaf1) have been found in many tumor types including leukemia and melanoma, as well as colon, gastric, and breast cancers (Lowe and Lin 2000; Johnstone et al. 2002).

Functional mutations or altered expression of Bcl-2 family members are also associated with cancer cell proliferation through a failure to induce apoptosis (Lowe and Lin 2000; Johnstone et al. 2002). In mammalian cells, fifteen Bcl-2 family members have been identified and consist of both repressors and inducers of apoptotic cell death (Lowe and Lin 2000). Bcl-2, itself, was originally characterized as a proto-oncogene because of its location on a breakpoint in human B-cell lymphomas, following chromosomal translocation (Kerr et al. 1994; Lowe and Lin 2000). Bcl-2 was later determined to inhibit apoptosis, rather than promote proliferation, in interleukin-3-depedent myeloid and lymphoid cell lines, following interleukin-3 deprivation (Ascaso et al. 1994; Kerr et al. 1994; Lowe and Lin 2000). Bcl-2 is an intrinsic repressor of apoptosis, and its overexpression has been significantly associated with both cancer development and metastasis, and has been estimated to occur in approximately half of all cancers (Bold et al. 1997; Johnstone

et al. 2002; Yip and Reed 2008). The inactivation or reduced expression of Bcl-2 family inducers of apoptosis, like Bax and Bak, result in an inability to suppress tumor growth by the induction of apoptosis, and have been identified in different tumor types, including colon, stomach, breast, gastric and hematopoietic cancers (Ouyang et al. 1998; Lowe and Lin 2000; Johnstone et al. 2002; Yip and Reed 2008; Kholoussi et al. 2014). Like p53, changes to the expression or function of Bcl-2 upstream components are associated with the dysregulation of apoptosis and result in tumorigenesis (Johnstone et al. 2002).

Disturbances to members of the extrinsic or death receptor apoptotic pathway are less common, although they have been found in tumor cells and result in an inability to undergo apoptosis following the binding of death receptors (Johnstone et al. 2002). Members of this pathway that commonly experience disruption include Fas receptor and TRAIL receptors 1 and 2 (Johnstone et al. 2002; Johnstone et al. 2008). Fas receptor, also known as Apo-1 or C95, is normally an extrinsic inducer of apoptosis and is responsible for the recruitment of the adaptor protein FADD and activation of membrane-proximal initiator caspases 8 and 10 (Lowe and Lin 2000; Johnstone et al. 2002; Johnstone et al. 2008). Since the proteolytic cleavage of caspase 8 results in the activation of its downstream components (e.g. caspases 3 and 7) in the extrinsic pathway or the activation of intrinsic pathway member Bid, functional mutations of this death receptor increases a tumor cell's resistance to apoptosis in either pathway (Johnstone et al. 2002). Autoimmune lymphoproliferative syndrome (ALPS) is a disorder marked by an inability to regulate the body's lymphocyte population due to a Fas receptor defect.

In this disorder, aberrant T-lymphocytes are able to evade apoptosis, and therefore, the frequency of lymphoma cancers in patients with ALPS is significantly increased (Johnstone et al. 2002). TRAIL receptor 1, otherwise known as Apo-2, and TRAIL receptor 2, are, like other members of the TNF receptor superfamily, responsible for the induction of apoptosis following the binding of extracellular ligands (e.g. TRAIL). Mutations in TRAIL receptors 1 and 2 and their downstream effectors (e.g. caspases 8 and 10) have been detected in a number of cancer types, including hematopoietic and breast cancers (Johnstone et al. 2008). In addition to encouraging tumorigenesis through the inhibition of apoptosis, alterations in extrinsic pathway death receptors appear to alter immune system surveillance, thereby promoting metastasis (Bold et al. 1997; Johnstone et al. 2002; Johnstone et al. 2008).

Apoptosis and Cancer Therapy

Traditional cancer therapy consists of a combination of surgery and cytotoxic agents, like chemotherapy and radiation. Surgery was first used to eliminate whole tumors, as well as lymph nodes, following the advent of anesthesia in the mid-nineteenth century (Sudhakar 2009). Medical imaging, like ultrasound and MRI, were developed in the 1970s, and improved the efficacy of tumor excision by reducing exploratory surgery (Sudhakar 2009). The use of cytotoxic agents, in combination with surgery, also greatly improved the effectiveness of cancer treatment (Sudhakar 2009). Chemotherapy, itself, was first used in the 1940s when researchers studied mustard gas and compounds related to it in order to develop better chemical warfare, as well as to develop better treatments against it (Sak

2012; American Cancer Society 2014). During this time, American pharmacologists, Louis Goodman and Alfred Gilman, reviewed the medical records of soldiers exposed to mustard gas in WWI and found that many of them suffered immune cell reduction (Sak 2012; Hazell 2014). In 1942, Goodman and Gilman administered mustard gas to a patient with lymphoma, after hypothesizing that if it has the capability to reduce normal immune cells, it should also be able to reduce cancerous ones. The administration of the mustard gas was found to alleviate some of the patient's discomfort (Hazell 2014). In 1948, Scottish chemist Alexander Haddow studied the component of mustard gas responsible for cytotoxicity and found that this component, called nitrogen mustard, induced cellular suicide with higher specificity than mustard gas (Hazell 2014). The use of radiation to treat cancer was discovered even earlier than chemotherapy, in 1896, when American scientist Emil Grubbe used radiation to treat a woman with breast cancer, and found that it briefly improved her condition (Markel 2015).

By the end of the 20th century, with more advanced surgical techniques, a larger variety of chemotherapeutic agents, and more precise delivery of chemotherapy and radiation (chemoradiation), cancer therapy had greatly improved (Sudhakar 2009). Traditional cancer therapies were further enhanced with increased understanding and evidence of the mechanisms responsible for cell death, as well as how these mechanisms were modified in different cancer types. Modern chemotherapy, therefore, came to be known as targeted cancer therapy. Targeted cancer therapy differs from traditional chemotherapy in that drugs, which can be cytostatic or cytotoxic, are designed or selected to act on specific molecular

targets, whereas traditional chemotherapy destroyed all cells to which it was administered (i.e. both healthy and cancerous cells) (National Cancer Institute 2014). Gene therapy is also often employed, alongside targeted cancer therapy, to increase the effectiveness of chemotherapeutic agents or to reestablish tumor sensitization to them.

Much of the current research on the relationship between apoptosis and cancer is concerned with the modifications in the pathways controlling apoptosis (e.g. p53) and how these can be utilized to improve targeted cancer and gene therapies (Lowe and Lin 2000). For example: Due to its involvement of p53 in apoptosis, many cancer treatments are concerned with targeting it with chemoradiation or restoring its function with gene therapy (Wang and Sun 2010). Traditional cancer therapies, like chemotherapy and radiation, are able to upregulate p53 by damaging cellular DNA and, therefore, increase apoptosis (Wang and Sun 2010). Since many cancer types are associated with mutations in p53, chemoradiation is often inappropriate and associated with drug resistance (Bold et al. 1997; Lowe and Lin 2000; Johnstone et al. 2002). Gene therapy allows the restoration of p53, and apoptosis, through viruses that reintroduce the wild-type allele or small molecules that bind to p53 and block the binding of its competitive inhibitors (Issaeva et al. 2004; Wang and Sun 2010). For instance, replication-deficient adenovirus (Ad-p53) was successfully used to reintroduce wild-type p53 to human lung cancer cells, and is now marketed under the brand name of Gendicine/Advexin for treatment of head, neck, and lung cancers (Wang and Sun 2010). ONYX-015 is an E1B-deleted adenovirus, currently in clinical trials, that

selectively replicates in and lyses cancer cells that do not express functional p53 (Wang and Sun 2010). RITA is the name of a small molecule that has been used to reactivate p53 by preventing the binding of Mdm2, an inhibitor of p53, as well as other repressors of apoptosis, including Mcl-1 and Bcl-2 (Issaeva et al. 2004; Wang and Sun 2010).

Vitamins and Cancer Therapy

The use of cancer therapies to upregulate p53 or modify its functionality, in order to induce apoptosis, provide evidence of the myriad possibilities that exist with both traditional and modern cancer treatments, as well as the challenges in integrating these approaches. Another emerging area of cancer research and integration is the use of vitamins and dietary metabolites, like vitamins C, D, E, and K, as primary or supplementary means of inducing apoptosis (Mathiasen et al. 1999; Sakagami et al. 2000; Sylvester 2007; Karasawa et al. 2013). Various types of vitamin K, for instance, have been shown to induce apoptosis and inhibit cell growth in a number of cancer types, including leukemia, lung, myeloma, and lymphoma, through the modification of members of both apoptotic pathways (Yaguchi et al. 1997; Yoshida et al. 2003; Tsujioka et al. 2006; Blair and Miller 2012). Vitamin K has also been used to enhance the apoptotic and inhibitory effects of pre-existing anti-cancer drugs, like Sorafenib, in pancreatic and liver cancers (Wei et al. 2010; Wei et al. 2010; Carr et al. 2011). The characterization and use of organic and nutritive compounds (like vitamin K) to induce apoptosis and inhibit cancerous cell growth is

appealing because of the resulting lack of damage to healthy cells, as well as the benefits to the immune system and implications for prevention (Mora et al. 2008).

Vitamin K. Vitamin K represents a class of fat-soluble, structurally similar vitamins that are known for their role as a cofactor in the post-translational modification (carboxylation) of proteins involved in blood coagulation and bone metabolism, which allows them to bind calcium ions, as well as in the regulation of cellular processes (Higdon 2000; Ehrlich 2013). Structurally, this group of vitamins is characterized by a naphthoquinone ring and a side chain consisting of 5-carbon units that vary in length, branching, and degree of unsaturation (Fieser et al. 1941; National Institute of Health 2015). There are two natural analogs of vitamin K – vitamin K1 (VK1) or phylloquinone and vitamin K2 or menaquinones (Higdon 2000). Phylloquinone is a phytochemical and metabolite of photosynthesis, where it functions as an electron carrier during photophosphorylation in chloroplasts (Marks 1975). Phylloquinone is primarily obtained through the dietary intake of higher order plants (National Institute of Health 2015). This analog of vitamin K is more saturated than menaquinones, containing only one double bond in its side chain, and is composed of the characteristic naphthoquinone ring and a four-unit side chain (Figure 1) (National Center for Biotechnology Information 2015). Menaquinones, in contrast, are a group of compounds that are synthesized by intestinal microbiota from animal products (i.e. meat, dairy), as well as fermented foods (Higdon 2000). Menaquinones consist of homologs that vary in the length of their unsaturated side chain and where each side chain unit contains a double bond,

and range from MK-2 through MK-14 (Higdon 2000; National Center for Biotechnology Information 2015; National Institute of Health 2015). Menaquinones are named according to the number of 5-carbon side chain units they contain, so that MK-4, for example, contains four side chain units (Higdon 2000). There are several types of synthetic vitamin K, with the most recognized being vitamin K3 or menadione (Higdon 2000; Council for Responsible Nutrition 2013). Menadione is a derivative of vitamin K, containing only the naphthoquinone ring, and is inactive until *in vivo* alkylation occurs (Higdon 2000; National Center for Biotechnology 2015). Unlike phylloquinone and menaquinones, the synthetic isomers of vitamin K, including menadione, are associated with toxicity (e.g. allergic reactions and hemolytic anemia) in large doses (Council for Responsible Nutrition 2013).

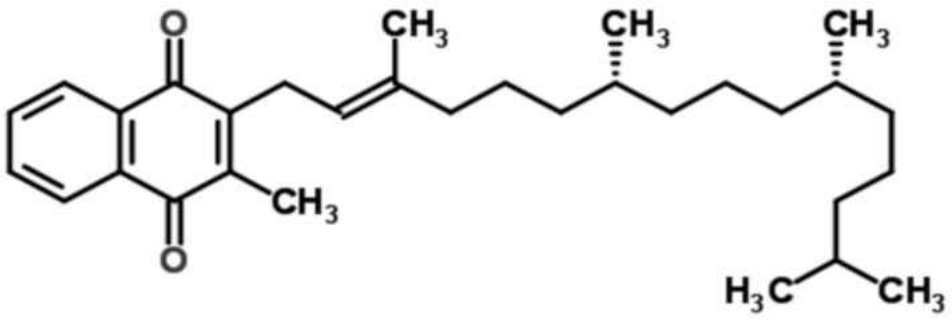

Figure 1: Structure of Phylloquinone. *2d chemical structure of phylloquinone or vitamin K1, IUPAC: 2-methyl-3-[(2E)-3,7,11,15-tetramethylhexadec-2-en-1-yl]napthoquinone (Source: ChemSpider).*

Phylloquinone, Apoptosis, and Cancer Therapy

Both natural analogs of vitamin K, phylloquinone and menaquinones, as well as synthetic menadione, have been shown to be involved in the induction of

apoptosis and inhibition of cancer cell growth, both *in vitro* and *in vivo* (Yaguchi et al. 1997; Yoshida et al. 2003; Hitomi et al. 2005; Criddle et al. 2006; Tsujioka et al. 2006; Zhang et al. 2006; Wei et al. 2010; Wei et al. 2010; Carr et al. 2011; Zhang et al. 2012; Karasawa et al. 2013; Suresh et al. 2013; Linsalata et al. 2015; Orlando et al. 2015). The apoptotic and anti-proliferative effects of phylloquinone have been examined in a number of cancer types, including colon, gastric, liver, and pancreatic (Wei et al. 2010; Wei et al. 2010; Carr et al. 2011; Linsalata et al. 2015; Orlando et al. 2015). One study examined these effects of phylloquinone in three colon cancer cell lines and found treatment with increasing concentrations of phylloquinone (10 μM to 200 μM) resulted in reduced cell growth and increased rates of apoptosis (Orlando et al. 2015). In addition, this study found phylloquinone modified the proliferative Ras/Raf/MEK/ERK pathway and significantly increased the ratio of Bax/Bcl-2 at concentrations of 100 μM or higher (Orlando et al. 2015). Another study looked at the effects of increasing concentrations of phylloquinone (10 μM to 200 μM) in gastric and colon cancer cell lines and found a concentration-dependent inhibition of cell proliferation and increased rates of apoptosis, particularly in colon cancer cells (Linsalata et al. 2015). This study also found decreased phosphorylation to members of the Ras/Raf/MEK/ERK pathway, as well as decreased polyamine biosynthesis, to be involved in these effects (Linsalata et al. 2015).

Two studies examined the effects of phylloquinone in combination with sorafenib, a small molecule tyrosine kinase inhibitor, and found the combined use of these compounds significantly elevated their apoptotic and inhibitory effects in both human and rodent hepatocellular carcinomas, compared to the separate use of both

compounds (Wei et al. 2010; Carr et al. 2011). These studies found the separate use of phylloquinone and sorafenib decreased phosphorylation of the calcium-dependent Ras/Raf/MEK/ERK pathway, upregulated p53, and increased the localization of several intrinsic inducers of apoptosis, including Bak and Bax, however, using these compounds together significantly enhanced their anti-cancer molecular modifications (Figure 2) (McCubrey et al. 2007; Wei et al. 2010; Carr et al. 2011). In addition to synergistically increasing the anti-cancer effects of one another, these studies found that the dosage of sorafenib (2.5 μM) and phylloquinone (25 μM) could be reduced and still produce the same effects (Wei et al. 2010; Carr et al. 2011). Another study examined the ability of phylloquinone and sorafenib to induce apoptosis and inhibit cell growth, both alone and combination, in pancreas adenocarcinoma cell lines, and found the separate use of these compounds produced insignificant anti-cancer effects, but when used in combination, there was a strong association with apoptosis and cell growth inhibition (Wei et al. 2010). This study also found that the combined use of phylloquinone and sorafenib activated effector caspase 3, initiator caspase 8, and intrinsic inducer of apoptosis, Bid, as well as inhibited proliferative pathway, Ras/Raf/MEK/ERK (Wei et al. 2010). Lastly, this study again found that by combining phylloquinone and sorafenib, they could reduce the dosage of each compound (2.5 μM and 25 μM, respectively) and still produce the same effects (Wei et al. 2010).

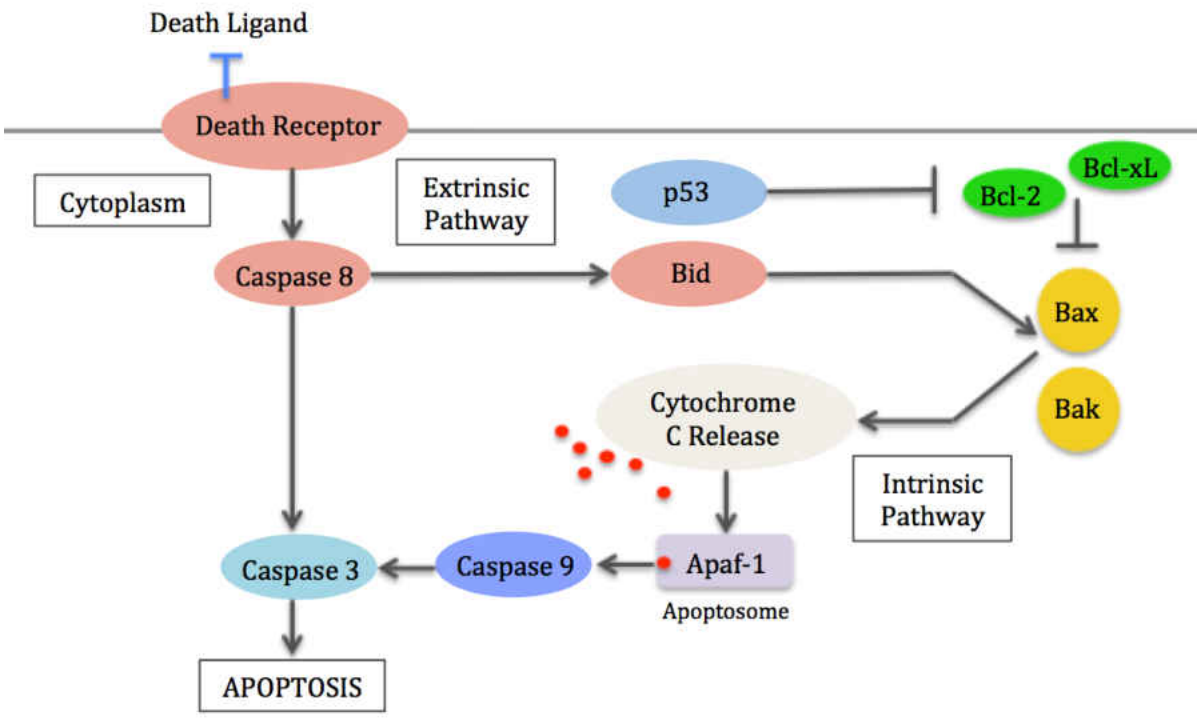

Figure 2: Members of the Intrinsic and Extrinsic Apoptotic Pathways Affected by Phylloquinone in Liver and Pancreatic Cancers. *Some members of the intrinsic or mitochondrial and extrinsic or death receptor pathway that have been shown to be modified following treatment with phylloquinone, alone or in combination with Sorafenib – a small tyrosine kinase inhibitor (*McCubrey et al. 2007; Wei et al. 2010; Wei et al. 2010; Carr et al. 2011; modified from Panayi et al. 2013).

These studies document the apoptotic and inhibitory effects of phylloquinone, whether used alone or in combination with an anti-cancer drug, and in doing so, demonstrate its chemotherapeutic and cytotoxic potential. There are, however, a fundamental lack of studies validating these effects, when compared to the chemotherapeutic utilization of menaquinones and menadione, and therefore, further characterization of phylloquinone is needed. Exploring the anti-cancer effects of phylloquinone could provide us with a better understanding of the mechanisms governing apoptosis and how tumor cells are able to modify these

mechanisms to promote tumorigenesis and metastasis. In addition, further characterization of phylloquinone would help to support its ability to enhance apoptosis and diminish cancer cell growth, and may lead its use as an anti-cancer drug, alone or in combination with other regulators of these processes.

Hypothesis, Rationale, and Specific Aims

This study seeks to verify the apoptotic and inhibitory effects of phylloquinone in a non-Hodgkin lymphoma cell line, known as U937. Through the examination of preliminary data and pertinent literature, the following hypotheses were made: (1) Treatment with phylloquinone will increase the frequency of apoptosis. (2) Treatment with phylloquinone will result in U937 cells with larger areas, which is attributed to membrane blebbing or macrophage differentiation (Blair and Miller 2012). (3) Treatment with phylloquinone will have an anti-proliferative effect on U937, resulting in decreased cell density. (4) Higher concentrations of phylloquinone and longer treatment times will enhance these effects, resulting in greater rates of apoptosis, less remaining viable U937 cells, and cells with even larger areas. These hypotheses are based on a preliminary study that was conducted in 2012, in which I a concentration-dependent reduction in U937 was observed and attributed to the induction of apoptosis. An increase in cell area was also observed and attributed to an increase in membrane blebbing and macrophage differentiation, as a result of apoptosis (Blair and Miller 2012). These experiments will be replicated and modified, in order to verify the occurrence of apoptosis.

This study will examine the ability of phylloquinone to reduce U937 cell growth through the induction of apoptosis in both a concentration- and time-dependent manner, in order to better characterize its effects, as well as to establish an experimental protocol. The effects of phylloquinone will be assessed through the quantification of U937 cell density and area, as well as through the use of molecular markers for apoptotic cell death to both verify and quantify its occurrence. The results of this study will provide evidence of the anti-cancer potential of phylloquinone, as well as will provide insight into its effects in a non-Hodgkin lymphoma cell line.

CHAPTER 2

MATERIALS AND METHODS

Experimental Design

The first aim of this study was to repeat the preliminary experiment, in order to verify the concentration-dependent reduction in U937 cell numbers, following treatment with several concentrations of phylloquinone (Blair and Miller 2012). In order to accomplish this, a series of experiments using the same parameters as the first study, such as treatment concentrations of 0, 10, 50, 100, or 500 μM phylloquinone and a treatment time of 7 days, were conducted (Table 1). Cell densities were determined for each control or treatment group. The second aim of this study was to establish an experimental protocol, in regards to phylloquinone concentration and treatment duration. This was accomplished by conducting several time series experiments, in which U937 densities were determined every 24 hours for 4 days (Table 1). In addition, a narrower range of treatment concentrations (0, 100, or 500 μM) was selected. These experiments led to selection of a 48-hour treatment time, as well as the continued use of 100 or 500 μM phylloquinone, for all future experiments (Table 1). The third aim of this research was to show that phylloquinone does induce apoptosis, as well as to show that this type of cell death is responsible for the resulting effects on cell density and area. To complete this, immunofluorescence assays were utilized to label cell surface and nuclear markers for apoptosis, which allowed the classification of individual cells as 'apoptotic' or 'non-apoptotic' (Table 1). Overall cell densities were determined at

the conclusion of each experiment. Afterwards, cells were incubated with fluorescently conjugated antibodies, wet mounted onto slides, and photographed. U937 cell areas were determined from these photographs. The fourth aim of this research was to demonstrate that higher concentrations of phylloquinone increase the frequency of apoptosis. This was completed by examining the proportion of cells labeled apoptotic from random field view photographs taken during immunofluorescence. Further details on experimental methodology and analysis are provided below.

No.	Date	Duration (days)	No. of Samples	No. of Concentrations	Description
1	5-23-14	7	10	4	Cell Density
2	6-9-14	7	10	4	Cell Density
3	7-11-14	4	3	2	Cell Density, Time Series
4	8-1-14	4	3	2	Cell Density, Time Series
5	8-1-14	7	12	4	Cell Density
6	9-10-14	4	3	2	Cell Density, Time Series
7	10-1-14	2	6	2	Cell Density, Cell Area
8	11-3-14	2	6	2	Cell Density, Cell Area
9	2-7-15	2	12	2	Cell Density
10	2-9-15	2	12	2	Cell Density
11	3-10-15	2	6	2	Cell Density, Cell Area, Annexin V
12	5-18-15	2	6	2	Cell Density, Cell Area, Annexin V
13	8-5-15	2	6	2	Cell Density, Cell Area, APO-BrdU
14	8-13-15	2	6	2	Cell Density
15	8-24-15	2	6	2	Cell Density
16	8-28-15	2	6	2	Cell Density, Cell Area, APO-BrdU
17	9-24-15	2	6	2	Cell Density, Cell Area, APO-BrdU
18	9-24-15	2	6	2	Cell Density, Cell Area, Annexin V

Table 1: Experiment List. *List of experiments (N = 18) containing the date, duration, number of samples, number of phylloquinone concentrations, and a description of the type of data collection – cell density, area, and/or the occurrence of apoptosis (i.e. annexin V or APO-BrdU).*

U937 Cell Line and Cell Culture

U937 cells were provided by the American Type Culture Collection (ATCC, Manassas, VA, United States). U937 were isolated from a histiocytic pulmonary or non-Hodgkin lymphoma of a 37-year-old Caucasian male (Sundström and Nilsson 1976; Sigma-Aldrich 2015). This non-adherent cell line exhibits the morphology of monocytes, but is capable of adopting the morphology of macrophages (Figure 3) (Passmore et al. 2001; Sigma-Aldrich 2015). U937 cells were maintained and cultured in RPMI-1640 with L-glutamine and sodium bicarbonate (Fisher Scientific, United States). Cell media was supplemented with 20% fetal bovine serum (FBS) (Sigma-Aldrich, United States). U937 cells were subcultured on a weekly basis at a 1:5 ratio of cells to media for a total volume of 30 ml per culture flask. All cell cultures were incubated and maintained at 37°C and 5% CO_2.

Experimental Culture Conditions

Cell culture experiments were set-up with an initial cell density of 1 x 10^5 or 2 x 10^5 cells/ml, depending on the particular experiment (Table 1). Cell stock densities were obtained via hemocytometer counts and adjusted to the specified concentration by diluting with supplemented media containing the appropriate concentration of phylloquinone (0, 10, 50, 100, or 500 μM). Cell media containing phylloquinone was diluted from a stock solution of 500 μM phylloquinone in 0.5% ethanol and supplemented cell media (RPMI-160 with 20% FBS) (see "Phylloquinone Solution", below). Cells were cultured in 12-well culture plates, with

a total volume of 3 ml of solution per well and incubated at 37°C and 5% CO_2 for 24 hours to 7 days, depending upon the experiment (Table 1).

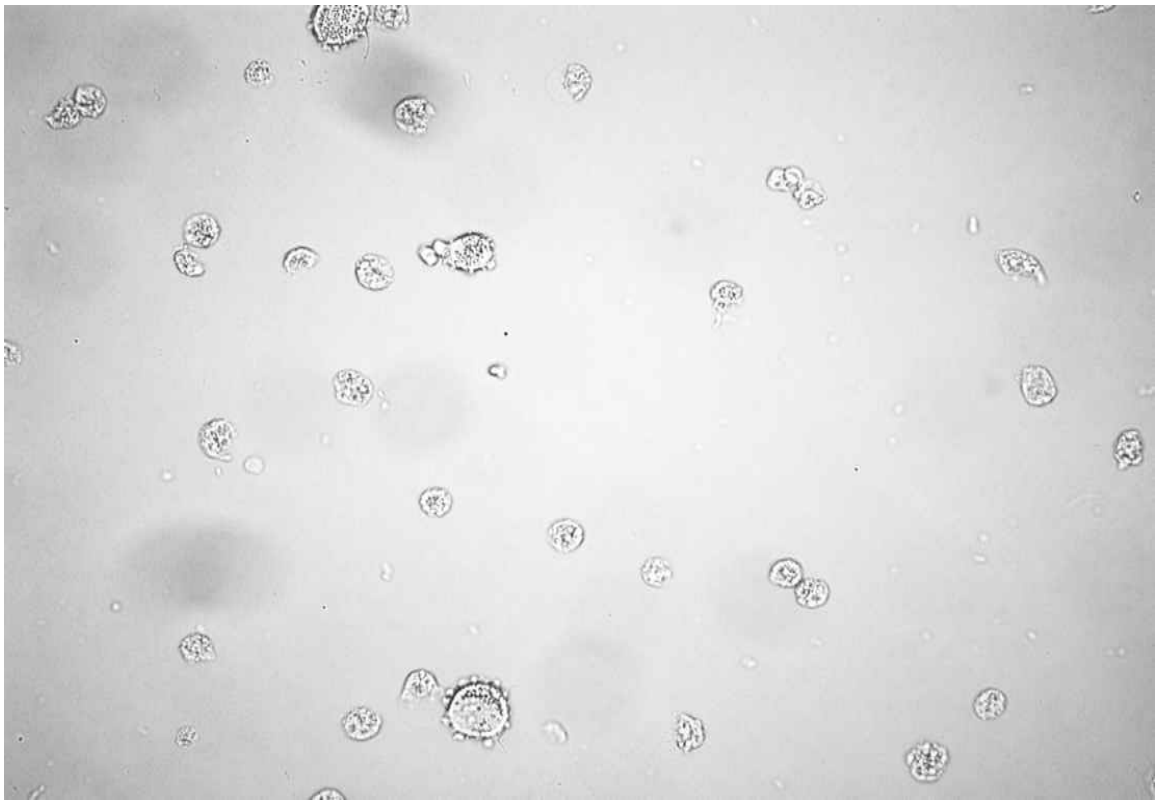

Figure 3: U937 cells at 20x magnification. *Image of wet mount of untreated U937 cells at 20x magnification. The majority of the cells in this image exhibit the morphology of monocytes, while several exhibit the morphology of macrophages.*

Phylloquinone Solution

A 500 µM phylloquinone stock solution was prepared by dispensing 4.6 µl phylloquinone (Sigma-Aldrich, United States) into 100 µl of ethanol and 2 ml of pre-warmed media (37°C) supplemented with FBS. This solution was briefly vortexed and diluted to 20 ml with additional warmed media. A 7 ml aliquot of 500 µM phylloquinone stock was transferred to a 15 ml conical tube and stored in a water

bath at 37°C until plating. Other concentrations of phylloquinone were made by diluting aliquots of the 500 µM stock solution to the appropriate concentration of phylloquinone (10, 50, or 100 µM) with 37°C supplemented media, for a total volume of 7 ml per each treatment concentration (Table 2). An aliquot of media containing 0 µM phylloquinone was created by diluting 35 µl of ethanol to 7 ml with pre-warmed RPMI-1640 supplemented with 20% FBS. Each aliquot was stored at 37°C until use.

Phylloquinone Concentration (µM)	Volume of 500 µM Stock (ml)	Volume of Supplemented Media (ml)
0	0.00	6.97*
10	0.14	6.86
50	0.70	6.30
100	1.40	5.60
500	7.00	0.00

Table 2: Phylloquinone Treatment Solution. *Composition of phylloquinone solution by volume of 500 µM stock and supplemented media for each treatment concentration, for a total of 7 ml per concentration. * The difference in volume in the control (0 µM) is due to the presence of ethanol (35 µl).*

Cell Culture Preparation

After establishing U937 cell stock density with hemocytometer counts, the appropriate volume of cell stock needed for 7 ml of solution with 1 x 10^5 or 2 x 10^5 cells/ml was calculated. This volume was pipetted first from the 7 ml aliquot of supplemented media intended for the control U937 group and replaced with the same volume of U937 cell stock. The cell-media aliquot was homogenized by inversion and 3 ml of this solution was dispensed into each control well. This

procedure was repeated for each treatment group, until all culture wells contained 3 ml of U937 at the calculated density, with 0, 10, 50, 100, or 500 μM phylloquinone in supplemented media. The U937 stock culture flask and cell-media aliquots were gently inverted between pipetting to ensure homogenization.

Data Collection

Cell Density and Area Determination

U937 cell densities were determined at the end of each experiment using a hemocytometer (Figure 4). Eight counts were conducted per control or treatment group, and averaged. Care was taken to homogenize the culture plate before sampling. U937 cell areas were determined by photographing wet mounted slides of each group and measured using an image analysis program, called ImageJ, U.S. National Institutes of Health, Bethesda, Maryland, USA, http://imagej.nih.gov/ij/. Cell areas were also determined following immunofluorescence assay (see "Determination of Apoptosis", below). For non-assayed cell areas, four random bright-field images were taken at 20x magnification (Figure 4). For assayed cells, each image was taken twice – once using fluorescence microscopy and once using bright-field microscopy – in order to distinguish between apoptotic and non-apoptotic cells. Fluorescent photographs were taken using the green excitation filter. The red excitation filter was also used to view the cells to ensure they were not auto-fluorescing. As before, four random images of each slide were taken at 20x magnification. Care was taken to minimize the amount of time each slide was

exposed to light to avoid photobleaching. Overall, apoptotic, and non-apoptotic U937 cells were measured and distinguished between using ImageJ. To do this, ImageJ was calibrated to a known distance at 20x magnification. The freehand lasso tool was then used to select the perimeter of each cell in an image. Overall cell areas were measured and analyzed by treatment group, as well as separately on the basis of fluorescence (where applicable), which was used as an indicator of apoptosis.

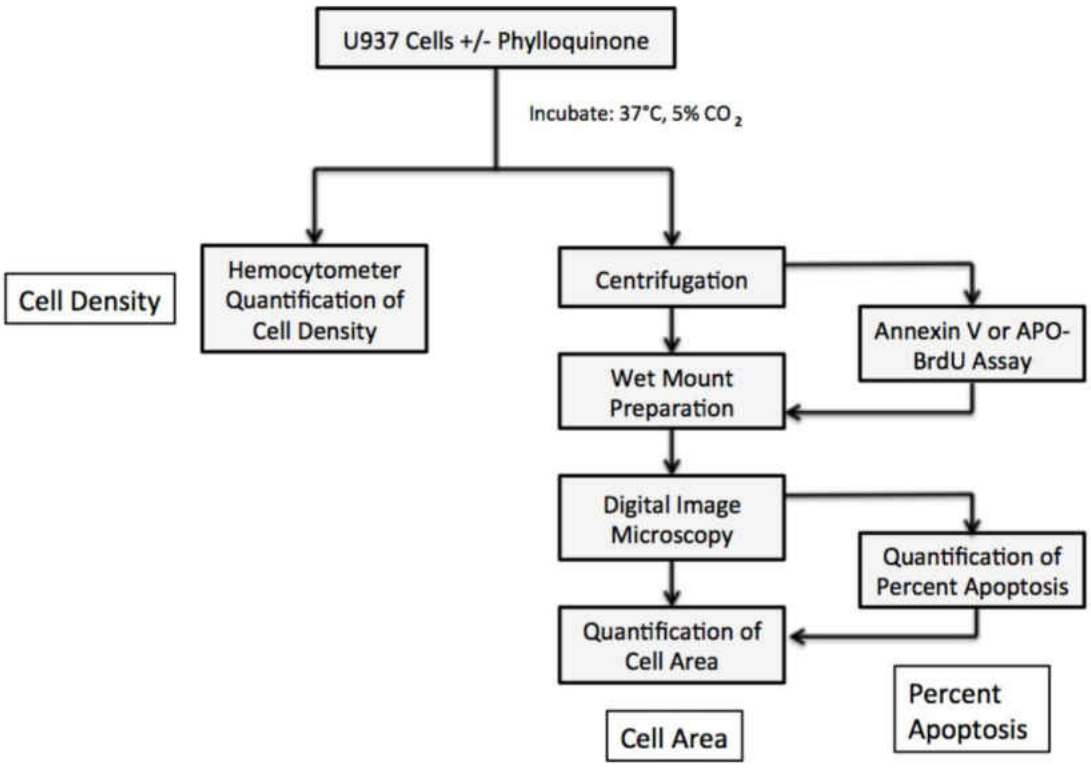

Figure 4: Cell Density, Cell Area, and Percent Apoptosis Flowchart. *Flowchart outlining U937 cell density, cell area, and percent apoptosis determination.*

Determination of Apoptosis

Apoptotic U937 cells were labeled using either the Annexin V-FITC Apoptosis Detection Kit (Sigma-Aldrich, United States) or APO-BrdU™ TUNEL Assay Kit, with Alexa Fluor® 488 Anti-BrdU (Sigma-Aldrich, United States) (Figure 5). Both assays utilize fluorescently conjugated antibodies to visualize biochemical changes characteristic of apoptosis. The annexin V protein was provided as part of the Annexin V FITC Apoptosis Detection Kit, which labels phosphatidylserine residues with annexin V conjugated to Alexa Fluor® 488. Phosphatidylserine is a phospholipid that is translocated from the inner-to-outer cell membrane early on in apoptosis. Annexin V has a high binding affinity for phosphatidylserine and binds to it preferentially, emitting fluorescence at the cell's surface that is detectable under UV light (van Engeland et al. 1998). The BrdUTP substrate and antibody were supplied with the APO-BrdU™ TUNEL Assay Kit. BrdUTP is a substrate that binds to 3'-hydroxyl ends of DNA, which are exposed following fragmentation in late stage apoptosis. The anti-BrdU anti-body included in this kit is fluorescently labeled with Alexa Fluor® 488 and binds to BrdUTP with high affinity, emitting nuclear fluorescence that is detectable under UV light (ThermoFisher Scientific 2015).

Annexin V Assay. The Annexin V-FITC Apoptosis Detection Kit was used to label apoptotic cells according to the following procedure (Figure 5). Following cell density determination, the contents of each well were collected and dispensed into separate 15 ml conical tubes. Each well of the culture plate was rinsed with 3 ml of cold (4°C) phosphate-buffered saline (PBS) and this was also dispensed into the

appropriate tube. These were centrifuged at 1000 rpm for 5 minutes. Once pelleted, the supernatant was poured off and the cells were washed in 1 ml of cold PBS, transferred to 1.5 ml microcentrifuge tubes, and re-pelleted by centrifugation at 1000 rpm for 5 minutes. The Annexin V Incubation Reagent was prepared by combining 10 µl of 10X Binding Buffer, 1 µl of Annexin-V conjugate, and 79 µl of deionized water, per cell sample. Care was taken to minimize reagent light exposure, and all components were stored on ice. Each sample was resuspended in 90 µl of reagent and incubated in the dark for 15 minutes at room temperature. The samples were then centrifuged for 5 minutes at 1000 rpm, pelleted, and washed with room temperature 0.5 ml 1X Binding Buffer, which was diluted from 10X Binding Buffer with deionized water. Following centrifugation, cells were resuspended in 100 µl of Binding Buffer and separately wet mounted to glass microscope slides. Glass coverslips were applied and slides were allowed to sit for several minutes before being transferred to the microscope. Samples were viewed and photographed within 2 hours.

APO-BrdU Assay. The APO-BrdU™ TUNEL Assay Kit was used to label apoptotic cells according to the following procedure (Figure 5). Following density determination, the contents of each well were collected as described above ("Annexin V Assay"). The samples were centrifuged at 1000 rpm for 5 minutes and resuspended in 5 ml of 1% paraformaldehyde (PFA) in PBS. Cells were fixed on ice for 5 minutes. The samples were then centrifuged for 5 minutes at 1000 rpm and washed in 5 ml of cold (4°C) PBS. This wash was repeated and each sample was

resuspended in 0.5 ml of PBS. To each test tube, 5 ml of ice-cold 70% ethanol was added. Cells were stored overnight at -20°C. The following day, the samples were allowed to come to room temperature and centrifuged at 1000 rpm for 5 minutes. Each sample was resuspended in 1 ml of wash buffer, transferred to 1.5 ml microcentrifuge tubes, and centrifuged at 1000 rpm for 5 minutes. This wash was repeated. The DNA-labeling solution was prepared by combining 10 µl of reaction buffer, 0.75 µl of TdT enzyme, 8.0 µl of BrdUTP, and 31.25 µl of deionized water, per cell sample. Each sample was resuspended in 50 µl of this solution and incubated for 60 minutes in a water bath at 37°C. Care was taken to invert the samples every 15 minutes, in order to keep the cells in suspension. Following incubation, 1 ml of rinse buffer was added to each sample and these were centrifuged at 1000 rpm for 5 minutes. This wash was repeated. The antibody staining solution was prepared by combining 5.0 µl Alexa Fluor® 488 dye-labeled anti-BrdU antibody with 95 µl of rinse buffer, per cell sample. Care was taken to minimize reagent light exposure, and all components were stored on ice. Each sample was resuspended in 100 µl of this solution and incubated for 30 minutes in the dark at room temperature. Following incubation, the contents of each tube were wet mounted to glass microscope slides. Glass coverslips were applied and slides were allowed to sit for several minutes before being transferred to the microscope. Samples were viewed and photographed within 2 hours.

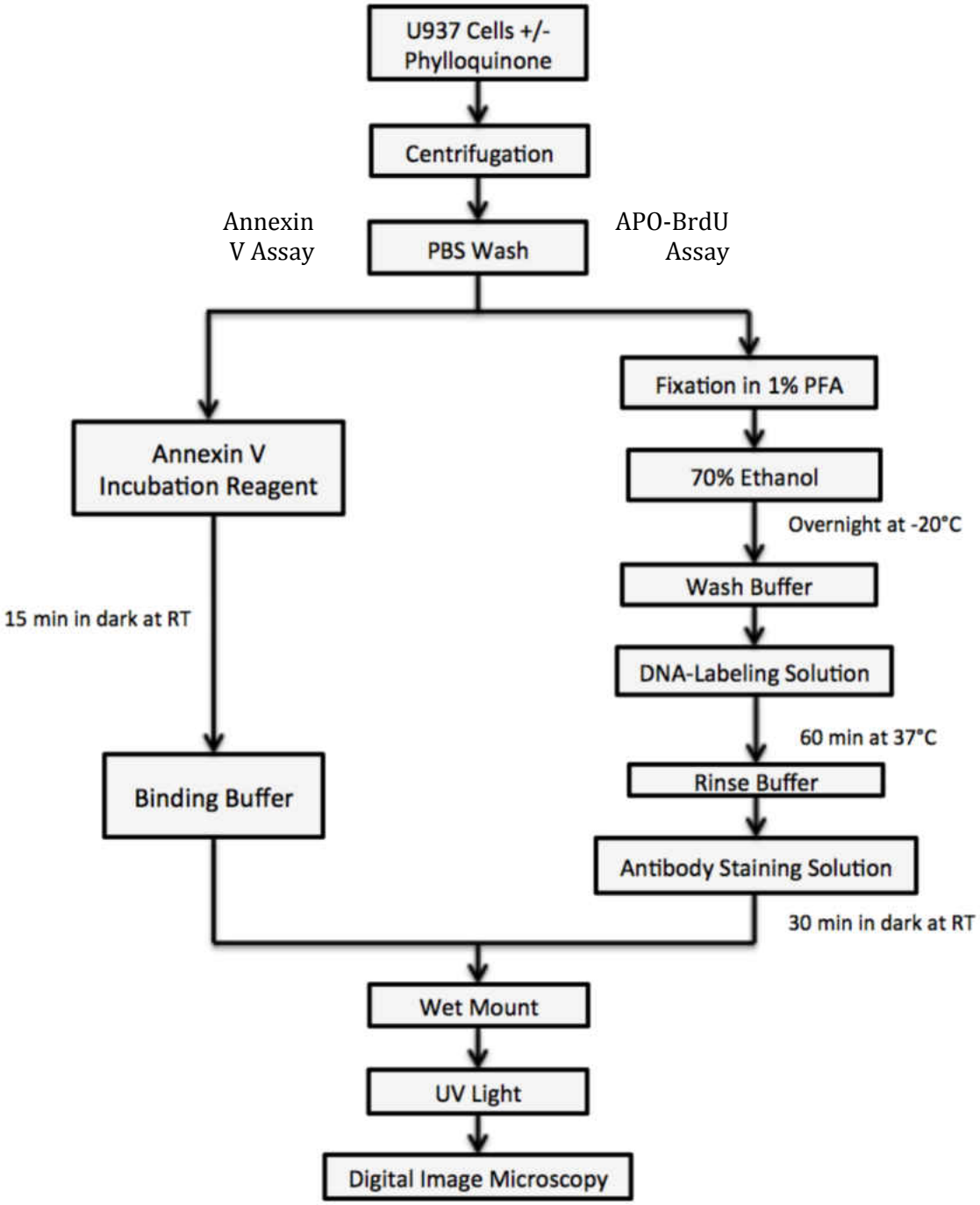

Figure 5: Annexin V and APO-BrdU Assay Flowchart. *Flowchart outlining the annexin V and APO-BrdU assay binding protocols used for these experiments.*

Analysis

Occurrence of Apoptosis Analysis

The occurrence of apoptosis was determined as a percent (Table 3). Percent apoptosis was calculated as the number of cells labeled with annexin V or APO-BrdU, relative to the total number of assayed cells, by treatment group.

Cell Area Analysis

GraphPad Prism version 6.00 for Windows, GraphPad Software, La Jolla, California, USA, www.graphpad.com and IBM SPSS software were used to analyze cell area data and create cell area figures (Figures 9 - 19). Cell areas were analyzed by treatment concentration, as well as between apoptotic or non-apoptotic groups, using a one-way analysis of variance (ANOVA). A one-way ANOVA was selected to test whether there is a significant difference between the variances of cell area (dependent variable) by treatment concentration (independent variable).

Cell Density Analysis

GraphPad Prism version 6.00 for Windows, GraphPad Software, La Jolla, California, USA, www.graphpad.com, Minitab, and IBM SPSS software were used to obtain statistics and create cell density figures (Figures 20 – 26). Cell densities were analyzed by treatment concentration and/or time, using a one- or two-way analysis of variance (ANOVA). A one-way ANOVA was selected to test whether there is a significant difference between the variances of cell density (dependent variable) by

treatment group (independent variable). A two-way ANOVA was selected to test whether there is a significant difference between the variances of cell density (dependent variable) by treatment concentration and time (independent variables).

CHAPTER 3

RESULTS

Occurrence of Apoptosis

The occurrence of apoptosis was determined for all assayed cells, following treatment with 0, 100, or 500 μM phylloquinone for 48 hours (Table 3). Apoptosis was examined as a percent. Percent apoptosis was calculated from the number of cells binding annexin V or APO-BrdU relative to the total number of assayed cells for that treatment group. The percent apoptosis for cells treated with 100 or 500 μM phylloquinone is 49.7% and 60.6%, respectively, while 8.5% of cells treated with no phylloquinone underwent apoptosis. This analysis also shows a concentration-dependent increase in the induction of apoptosis with increasing concentrations of phylloquinone, however, the rates of apoptosis increased by only about 10% with a fivefold increase in the concentration of phylloquinone. These results are based upon six experimental replicates, with three of each assay type (Annexin V or APO-BrdU) (Table 1).

Images of U937 cells treated with 0, 100, and 500 μM phylloquinone labeled with annexin V are shown below (Figure 6). Cells that are fluorescent, or positive for the binding of annexin V, are considered to be in the early stages of apoptosis. These images show treatment with 100 μM phylloquinone increases the frequency and intensity of the binding of annexin V, as well as reduces cell density and increases cell area. These images also show treatment with 500 μM phylloquinone enhances

these effects, resulting in higher and more intense binding of annexin V and even less remaining U937 cells with larger areas.

Phylloquinone Concentration (μM)	No. of annexin V binding cells	No. of APO-BrdU binding cells	Total number of apoptotic cells	Total number of cells	Percent apoptosis
0	17	57	74	867	8.5%
100	297	129	426	858	49.7%
500	309	219	528	871	60.6%

Table 3: Occurrence of Apoptosis Following Treatment with 0, 100, or 500 μM Phylloquinone for 48 Hours. *Percent apoptosis determined from the number of U937 cells binding annexin V or APO-BrdU relative to the total number of U937 by treatment concentration. Table contains number of annexin V or APO-BrdU binding U937 cells, as well as the total number of apoptotic cells, total number of measured cells, and percent apoptosis, following treatment with phylloquinone (0, 100, or 500 μM) at 48 hrs. Table represents the results of six different experiments (N=6).*

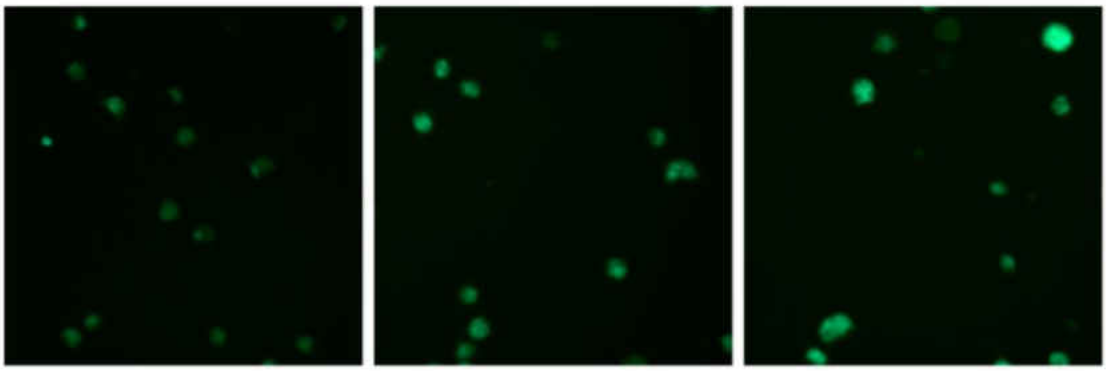

0 μM phylloquinone 100 μM phylloquinone 500 μM phylloquinone

Figure 6: U937 Cells Binding Annexin V Following Treatment with 0, 100, or 500 μM Phylloquinone for 48 Hours. *Images of U937 cells at 20x magnification following treatment with increasing concentrations of phylloquinone (0, 100 or 500 μM) at 48 hrs. Apoptotic cells are labeled with annexin V conjugated to Alexa Fluor 488.*

Cell Area

U937 cell areas were determined following treatment with 0, 100, or 500 μM phylloquinone for 48 hours (Figure 7, Table 1). Cell areas were analyzed on the basis of phylloquinone concentration, by apoptotic and non-apoptotic groups, and by assay type (i.e. Annexin V or APO-BrdU). Overall cell areas were determined from all experiments where cell areas were collected, without regard to apoptotic or non-apoptotic groups, and show a concentration-dependent increase in mean cell area following treatment with increasing concentrations of phylloquinone (Figure 7). The mean cell area of cells treated with no phylloquinone is 0.162 μm^2, while the mean cell areas of cells treated with 100 or 500 μM phylloquinone are 0.173 μm^2 and 0.199 μm^2, respectively. This data represents the results of eight experimental replicates. This data were analyzed using a one-way ANOVA. The results of this analysis indicate overall U937 area varies significantly between control and treatment groups, and increases with increasing phylloquinone concentrations ($F(2, 3020) = 12.994$, $p < 0.001$).

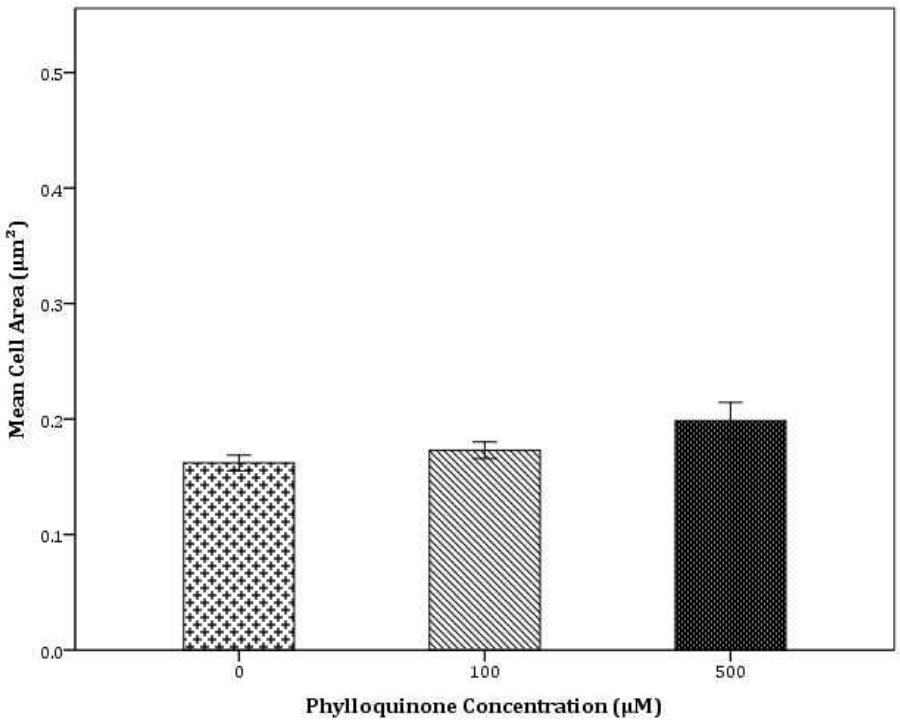

Figure 7: Mean Cell Area Following Treatment with 0, 100, or 500 µM Phylloquinone for 48 Hours. *Mean U937 cell area following treatment with increasing concentrations of phylloquinone (0, 100 or 500 µM) at 48 hrs. Data represents the results of eight different experiments (N = 8) (mean ± SEM). Data were analyzed by a one-way ANOVA (F (2, 3020) = 12.994, p < 0.001).*

The distribution of all U937 cell areas is unimodal and positively skewed, with areas ranging from 0.0 to 2.0 µm^2 (Figure 8). This distribution shows the majority of cells have areas that are concentrated to the left, with several outliers at 2.0 µm^2. The distribution of cell areas are shown for each concentration of phylloquinone (0, 100, or 500 µM) and these follow the same trend as mean cell area, in that, cells treated with phylloquinone are larger and occupy an area nearer to the right of the distribution, while untreated or control cells are smaller and occupy an area to the left of the distribution. In addition, cells treated with a higher concentration of phylloquinone (500 µM) have areas that are larger than cells

treated with a lower concentration of phylloquinone (100 µM). The range of cell area also varies between each group, with untreated cells exhibiting the most narrow spread (0.02 to 0.45 μm^2), and cells treated with the higher phylloquinone concentrations exhibiting progressively wider ones - 0.03 to 0.61 μm^2 for 100 µM phylloquinone and 0.04 to 2.0 μm^2 for 500 µM phylloquinone. This data represents the results of eight experimental replicates and indicates increasing concentrations of phylloquinone result in cells with larger areas.

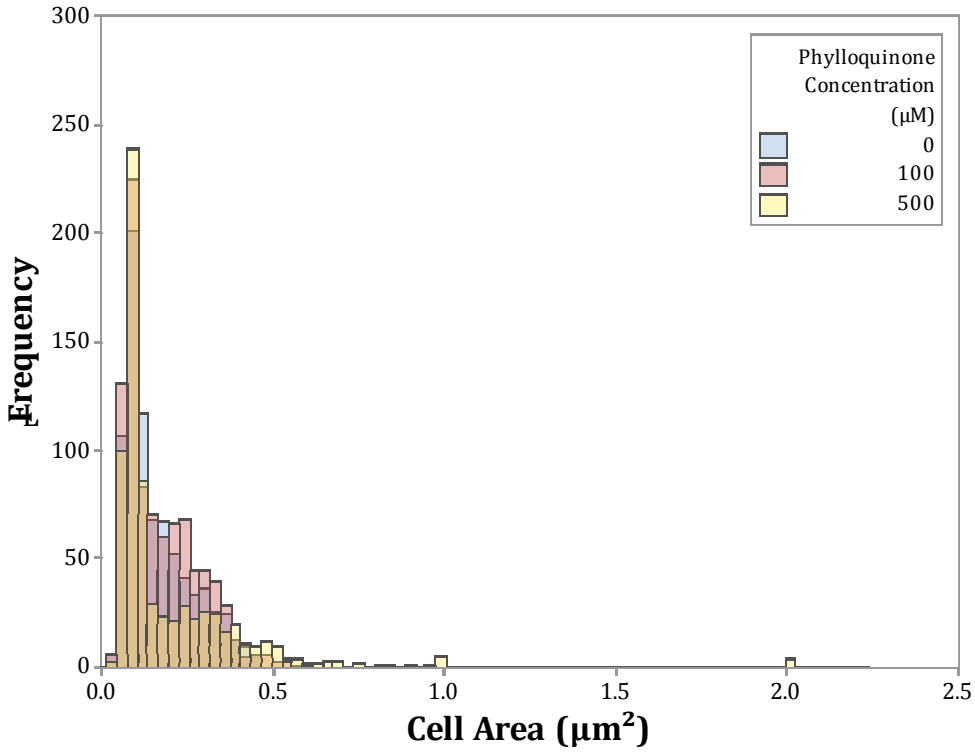

Figure 8: Distribution of Cell Area Following Treatment with 0, 100, or 500 µM Phylloquinone for 48 Hours. *Distribution of U937 cell area following treatment with increasing concentrations of phylloquinone (0, 100, or 500 µM) at 48 hrs. Data represents the results of eight different experiments (N = 8).*

U937 cell areas were also determined for both apoptotic and non-apoptotic cells following treatment with 0, 100, or 500 μM phylloquinone at 48 hours (Figures 9 - 19). Cells that were identified as apoptotic due to their binding of annexin V exhibit a concentration-dependent increase in cell area with increasing concentrations of phylloquinone, so that untreated apoptotic cells have the smallest mean area (0.091 μm^2), cells treated with a lower concentration of phylloquinone (100 μM) have the second largest mean area (0.098 μm^2), and cells treated with a higher concentration of phylloquinone (500 μM) have the largest mean area (0.108 μm^2) (Figure 9). This data represents the results of three experimental replicates. A one-way ANOVA was used to analyze mean areas of annexin V binding cells by treatment group. The results of this analysis indicate there is a significant difference between the mean areas of untreated and treated groups of early apoptotic U937 cells, as well as shows that the mean area of apoptotic U937 cells increases with increasing concentrations of phylloquinone ($F(2, 620) = 4.069$, $p < 0.05$).

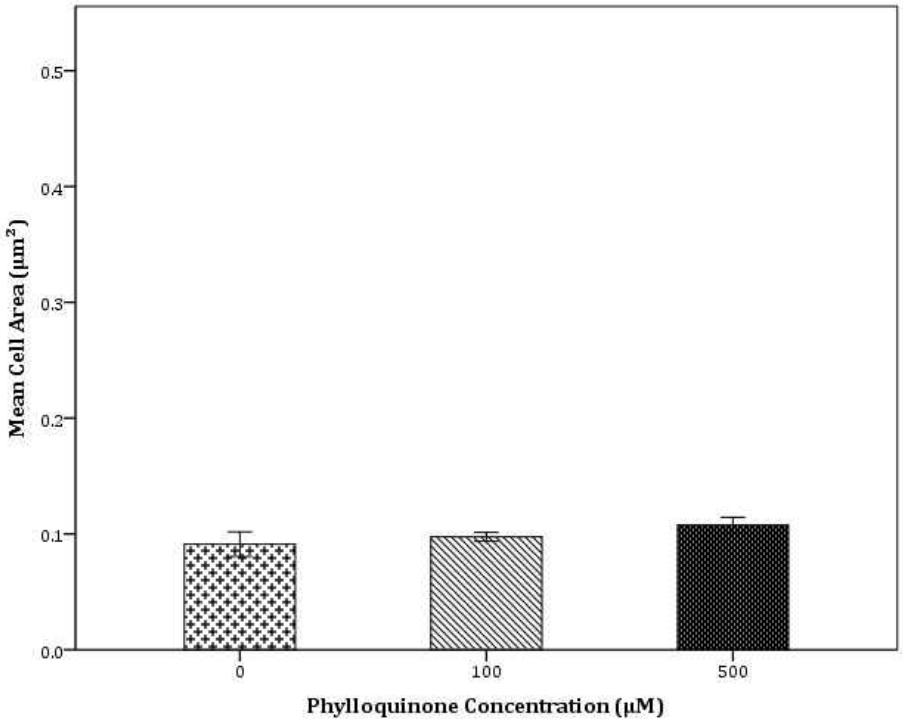

Figure 9: Mean Area of Annexin V Binding Cells Following Treatment with 0, 100, or 500 µM Phylloquinone for 48 Hours. *Mean area of annexin V binding U937 cells following treatment with increasing concentrations of phylloquinone (0, 100 or 500 µM) at 48 hrs. Data represents the results of three different experiments (N = 3) (mean ± SEM). Data were analyzed by a one-way ANOVA (F (2, 620) = 4.069, p < 0.05).*

The distribution of cells binding annexin V is unimodal and skewed to the right, with the majority of cell areas occupying the left of the distribution and areas that range from 0.04 to 0.40 µm^2 (Figure 10). Cells area distributions are shown relative to each concentration of phylloquinone (0, 100, or 500 µM) and follow the same pattern as overall cell areas, in that, with increasing concentrations of phylloquinone, the areas of early-stage apoptotic cells increase. The distribution of annexin V binding cells shows that untreated cells are the least frequent and have the smallest areas, while annexin V binding cells treated with 100 µM phylloquinone are more frequent and have larger areas, and cells treated with 500 µM

phylloquinone are the most frequent and have the largest areas. The range of annexin V binding cell areas also varies between treatment group, so that cells treated with 0 μM phylloquinone have the most narrow spread (0.05 to 0.12 μm^2), while cells treated with 100 μM have a wider range (0.04 to 0.22 μm^2) and cells treated with 500 μM have the widest range (0.05 to 0.40 μm^2). This data represents the results of three experimental replicates and indicates early-stage apoptotic cells have larger areas with increasing concentrations of phylloquinone.

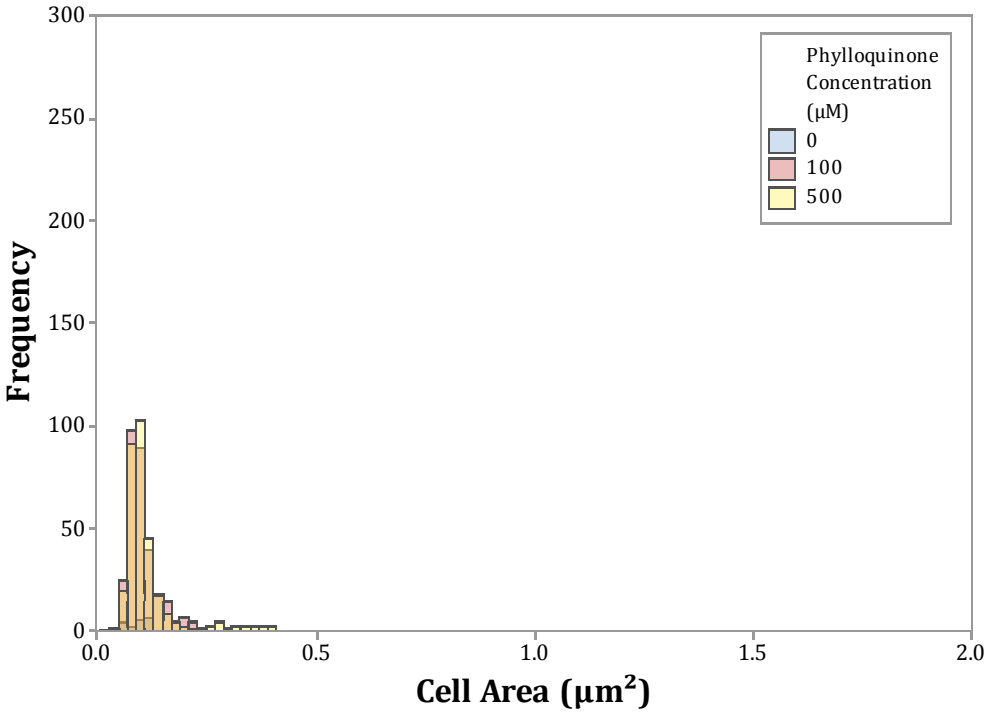

Figure 10: Distribution of Annexin V Binding Cell Area Following Treatment with 0, 100, or 500 μM Phylloquinone for 48 Hours. *Distribution of annexin V binding U937 cell area following treatment with increasing concentrations of phylloquinone (0, 100, or 500 μM) at 48 hrs. Data represents the results of three different experiments (N = 3).*

U937 cells that did not bind annexin V, and were thus identified as non-apoptotic, also increase in response to treatment with phylloquinone, as well as exhibit a concentration-dependent increase in cell area following treatment with higher phylloquinone concentrations (Figure 11). Mean cell areas reveal that non-apoptotic U937 cells treated with 0 μM phylloquinone have the smallest mean area (0.116 μm^2), while cells treated with 100 and 500 μM have larger areas (0.145 and 0.151 μm^2, respectively). This data was collected from three experimental replicates. A one-way ANOVA was used to analyze mean area of non-apoptotic U937 following treatment with phylloquinone. The results of this analysis suggest there is a significant difference between the mean area of non-apoptotic U937 cells treated with different concentrations of phylloquinone ($F(2, 1004) = 18.124$, $p < 0.001$).

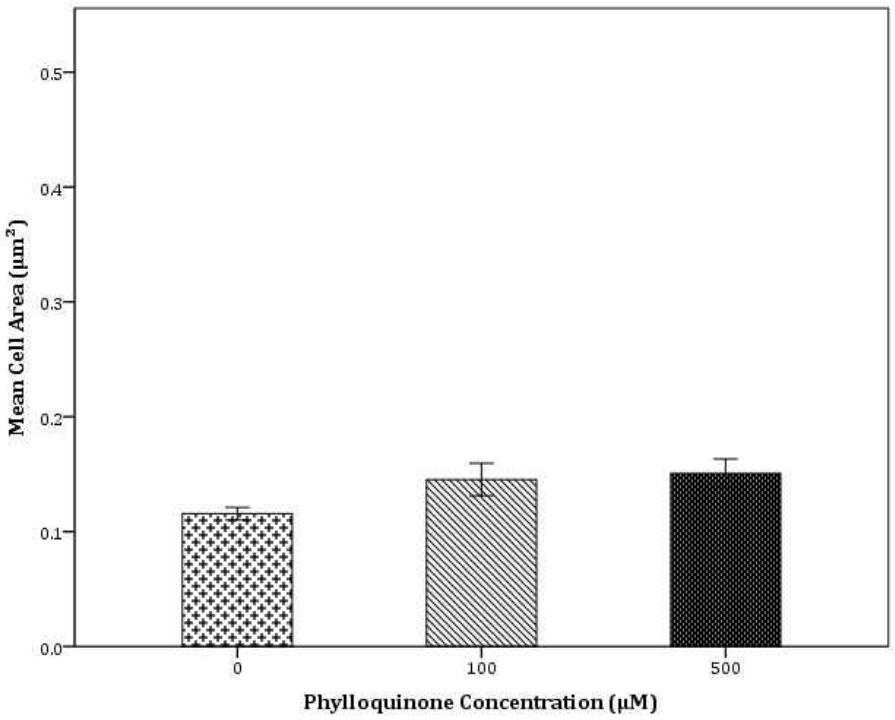

Figure 11: Mean Area of Annexin V Non-Binding Cells Following Treatment with 0, 100, or 500 µM Phylloquinone for 48 Hours. *Mean area of annexin V non-binding U937 cells following treatment with increasing concentrations of phylloquinone (0, 100 or 500 µM) at 48 hrs. Data represents the results of three different experiments (N = 3) (mean ± SEM). Data were analyzed by a one-way ANOVA (F (2, 1004) = 18.124, p < 0.001).*

The distribution of areas of U937 cells which did not bind annexin V, and were thus considered non-apoptotic, is unimodal and right-skewed, with areas ranging from 0.02 to 1.0 µm² (Figure 12). Again, the majority of areas are concentrated to the left of the distribution, with the areas of untreated cells confined to this region and the areas of cells treated with higher concentrations of phylloquinone progressing toward the right side of the distribution. In other words, this data follows the same trend established by preceding data, which is: the area of non-apoptotic U937 cells increases in the presence of phylloquinone, and is dependent upon concentration, so that higher concentrations of phylloquinone

further increase cell area. The distribution of non-annexin V binding cell areas also shows that while cells treated with the lower concentration of phylloquinone (100 μM) occupy a region that is further left in the distribution than cells treated with the higher concentration of phylloquinone (500 μM), however, the spread of cell area for the lower concentration is more variable. Cell areas of non-apoptotic U937 treated with no phylloquinone range from 0.02 to 0.60 μm^2, while those treated with 100 μM phylloquinone range from 0.03 to 1.0 μm^2 and 0.04 to 0.51 μm^2 for 500 μM. This data represents the represents the results of three experimental replicates, and shows that non-apoptotic cell area increases with exposure to phylloquinone, as well as increases in response to higher phylloquinone concentrations.

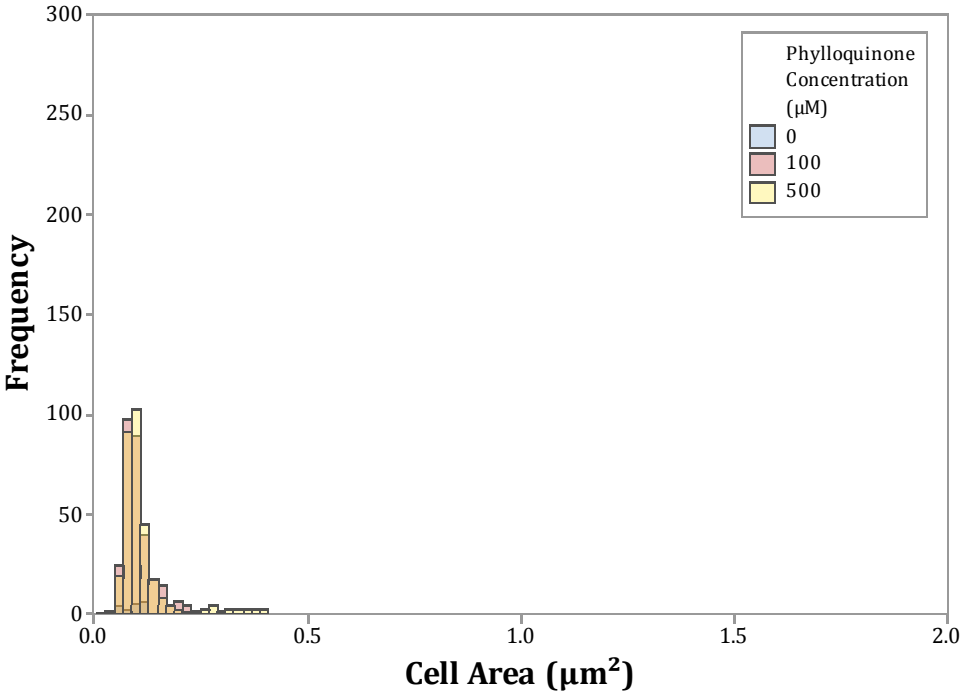

Figure 12: Distribution of Annexin V Non-Binding Cell Area Following Treatment with 0, 100, or 500 μM Phylloquinone for 48 Hours. *Distribution of annexin V non-binding U937 cell area following treatment with increasing concentrations of phylloquinone (0, 100, or 500 μM) at 48 hrs. Data represents the results of three different experiments (N = 3).*

U937 cell areas of cells that were identified as apoptotic based upon their binding of APO-BrdU demonstrate the same trend in the relationship between cell area and phylloquinone concentration, in that, the mean area of late-stage apoptotic cells increase in following treatment with phylloquinone, as well as further increase with increasing phylloquinone concentrations (Figure 13). The mean area of apoptotic control cells (0 μM) is the smallest (0.258 μm^2), while apoptotic cells treated with 100 μM have a larger mean area (0.270 μm^2), and cells treated with 500 μM phylloquinone have the largest mean area (0.414 μm^2). This data represents the results of three experimental replicates. A one-way ANOVA was used to analyze mean areas of APO-BrdU binding cells by phylloquinone concentration (0, 100, or 500 μM). The results of this analysis indicate treatment of U937 cells with phylloquinone increases apoptotic cell area, as well as that apoptotic cell area is dependent on the concentration of phylloquinone, so that increasing the treatment concentration results in increasing cell areas ($F(2, 402) = 14.390$, $p < 0.001$).

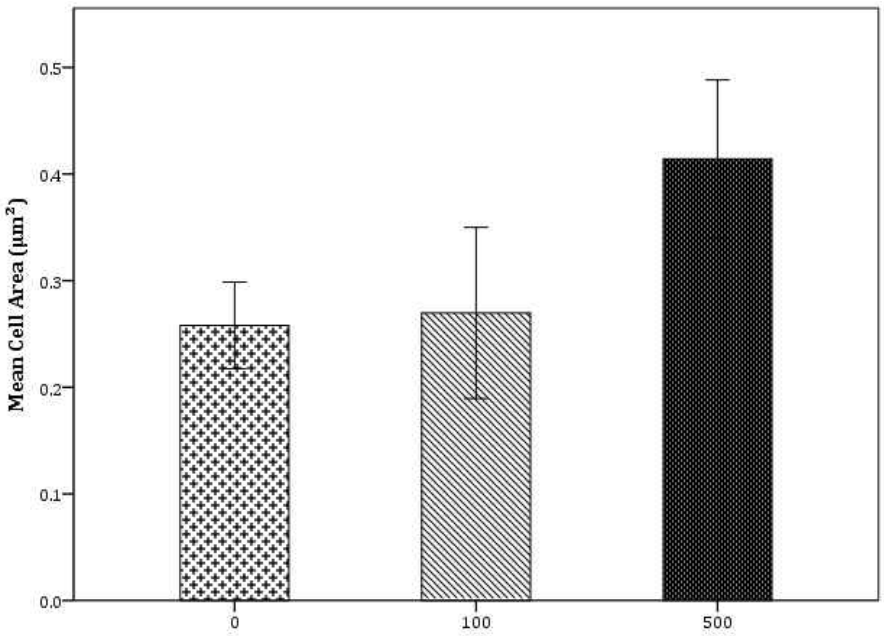

Figure 13: Mean Area of APO-BrdU Binding Cells Following Treatment with 0, 100, or 500 μM Phylloquinone for 48 Hours. *Mean area of APO-BrdU binding U937 cells following treatment with increasing concentrations of phylloquinone (0, 100 or 500 μM) at 48 hrs. Data represents the results of three different experiments (N = 3) (mean ± SEM). Data were analyzed by a one-way ANOVA (F (2, 402) = 14.390, p < 0.001).*

The distribution of U937 binding APO-BrdU cell area is unimodal and positively skewed, with the majority of cell areas occupying the left side of the distribution, while several outliers are represented to the right (Figure 14). The distribution of APO-BrdU binding cell areas range from 0.10 to 1.90 μm^2, and are shown for each phylloquinone concentration (0, 100, or 500 μM). Again, the distribution of APO-BrdU binding cells follows the same pattern as other datasets, in that untreated (0 μM) U937 cells are less frequent and have smaller areas (0.13 to 0.39 μm^2), while cells treated with the lower concentration of phylloquinone (100 μM) are more frequent and have larger areas (0.10 to 1.90 μm^2), and cells treated with the highest concentration of phylloquinone (500 μM) are the most frequent

and have the largest cell areas (0.10 to 1.90 μm^2). It is important to note that the range of apoptotic cell areas for U937 treated with the lower concentration of phylloquinone contains both the smallest and largest areas, meaning that, although the majority of apoptotic cells in this treatment group exhibit areas that are larger than the control and smaller than the highest treatment concentration, this group does contain a fair amount of variability. This data represents the results of three experimental replicates and indicates late-stage apoptotic cells are larger when treated with phylloquinone, as well as that their areas increase with increasing concentrations of phylloquinone.

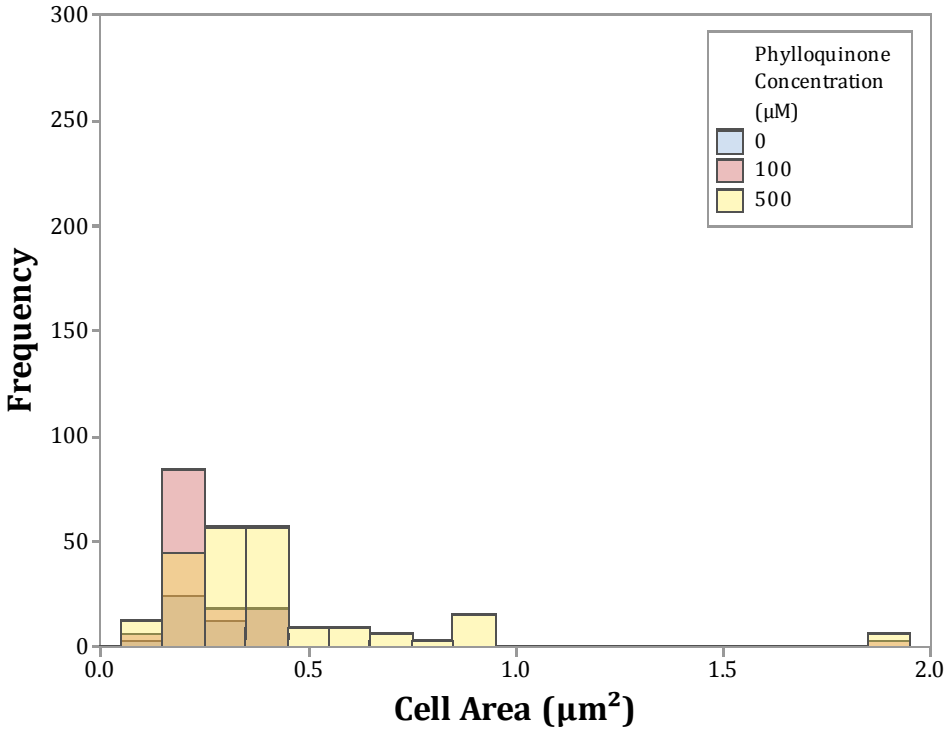

Figure 14: Distribution of APO-BrdU Binding Cell Area Following Treatment with 0, 100, or 500 μM Phylloquinone for 48 Hours. *Distribution of APO-BrdU binding U937 cell area following treatment with increasing concentrations of phylloquinone (0, 100, or 500 μM) at 48 hrs. Data represents the results of three different experiments (N = 3).*

U937 cells that did not bind to APO-BrdU, and were thus considered to be non-apoptotic, once again demonstrate the same increase in area, following treatment with increasing concentrations of phylloquinone (Figure 15). The mean cell area of non-apoptotic U937 treated with no phylloquinone is the smallest (0.237 μm^2), while the mean area of cells treated with 100 μM phylloquinone is the second largest (0.250 μm^2), and lastly, the mean area of cells treated with 500 μM phylloquinone is the largest (0.355 μm^2). This was collected from three experimental replicates. A one-way ANOVA was used to analyze the mean areas of APO-BrdU non-binding cells. The results of this analysis indicate there is a significant difference between the mean cell areas of each treatment group ($F(2, 558) = 31.082$, $p < 0.001$).

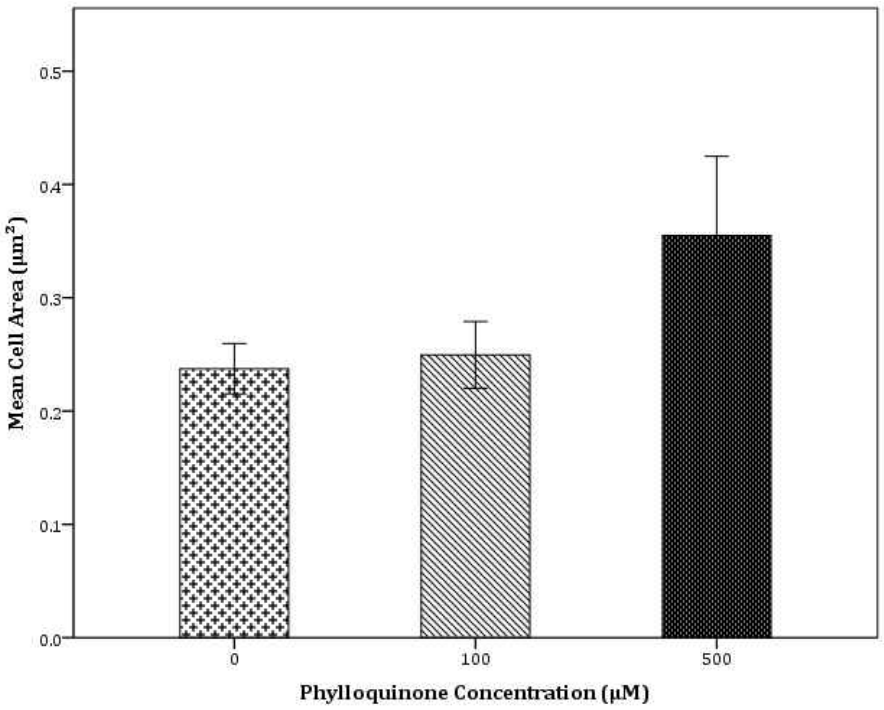

Figure 15: Mean Area of APO-BrdU Non-Binding Cells Following Treatment with 0, 100, or 500 µM Phylloquinone for 48 Hours. *Mean area of APO-BrdU non-binding U937 cells following treatment with increasing concentrations of phylloquinone (0, 100 or 500 µM) at 48 hrs. Data represents the results of three different experiments (N = 3) (mean ± SEM). Data were analyzed by a one-way ANOVA (F (2, 558) = 31.082, p < 0.001).*

The distribution of APO-BrdU non-binding U937 cell area is unimodal and skewed to the right, with the mass of cell areas occupying the left side of the distribution (Figure 16). The distribution of cell areas of APO-BrdU non-binding cells range from 0.01 to 0.89 µm^2, and are shown for each concentration of phylloquinone (0, 100, or 500 µM). This distribution conforms to other area distributions, in that the presence of phylloquinone produces non-apoptotic cells with larger areas, as well as that increasing concentrations of phylloquinone result in cells with increasingly larger areas. As before, untreated cells are the most frequent and occupy the left-most area of the distribution (0.01 to 0.47 µm^2), while

cells treated with 100 μM phylloquinone are less frequent and occupy an area of the distribution that is more toward the right (0.01 to 0.51 μm^2) and cells treated with 500 μM phylloquinone are the least frequent and occupy an area of the distribution that is furthest right (0.03 to 0.89 μm^2). Like most other area distributions, treatment with the highest concentration of phylloquinone result in cell areas with the greatest spread, while untreated cells exhibit the least amount of variation in cell area. This data represents the results of three experimental replicates and again demonstrates that treatment with phylloquinone increases cell area, regardless of a cell's apoptotic state. In addition, this data also shows that increasing the concentration of phylloquinone results in U937 cells with increasing area.

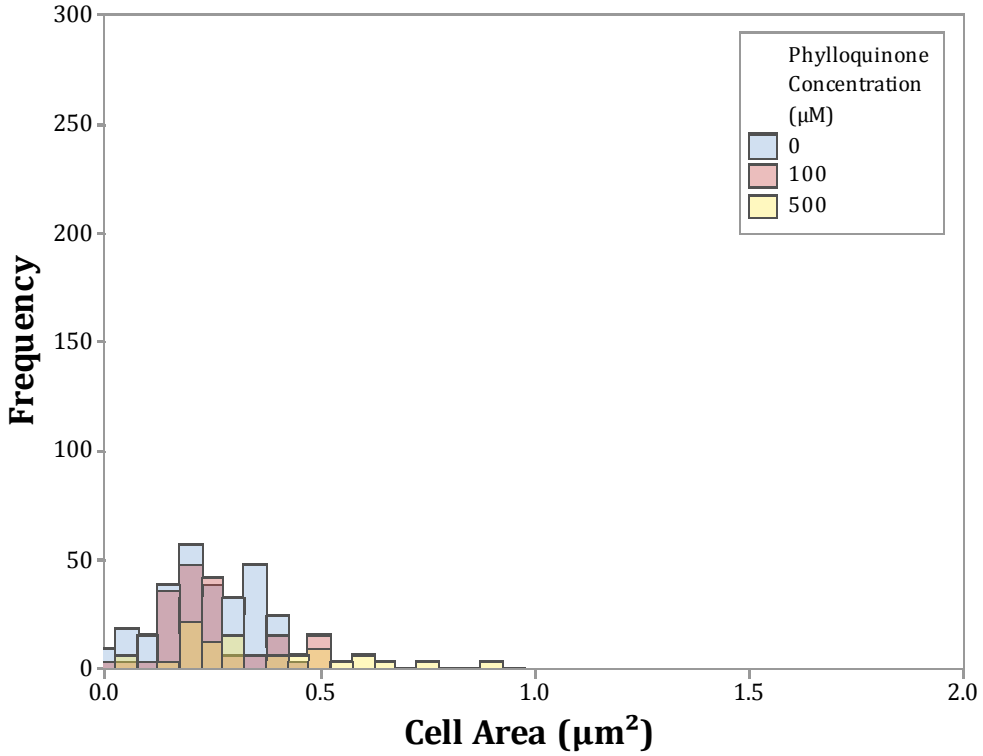

Figure 16: Distribution of APO-BrdU Non-Binding Cell Area Following Treatment with 0, 100, or 500 µM Phylloquinone for 48 Hours. *Distribution of APO-BrdU non-binding U937 cell area following treatment with increasing concentrations of phylloquinone (0, 100, or 500 µM) at 48 hrs. Data represents the results of three different experiments (N = 3).*

The distribution of both annexin V and APO-BrdU binding cell area, which were identified as apoptotic, is unimodal and positively skewed, with the majority of cell areas binding annexin V occupying the left side of the distribution and the majority of cell areas binding APO-BrdU occupying the right side of the distribution (Figure 17). This distribution suggests early-stage apoptotic cells, bound to annexin V, have smaller cell areas than late-stage apoptotic cells, bound to APO-BrdU. In addition, the spread of annexin V binding cell areas is narrower than the spread of

APO-BrdU binding cells, which indicates cells experiencing apoptosis vary less in size in during early apoptosis and more during late-stage.

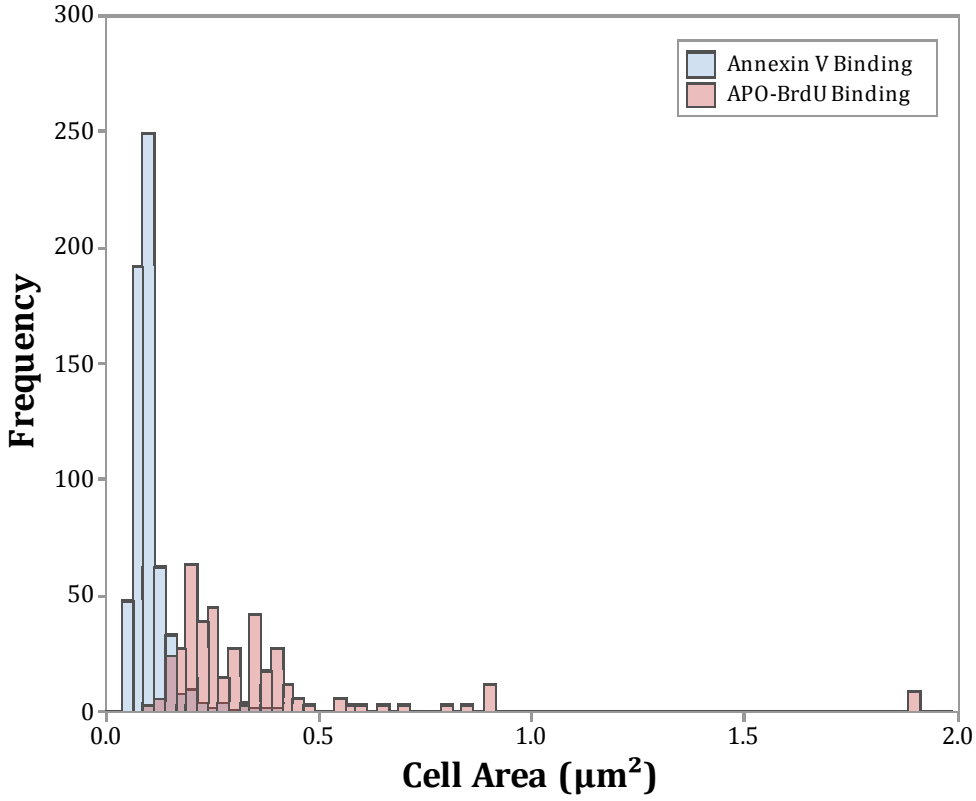

Figure 17: Distribution of Annexin V and APO-BrdU Binding Cell Area Following Treatment with 0, 100, or 500 µM Phylloquinone for 48 Hours. *Distribution of annexin V and APO-BrdU binding U937 cell area following treatment with increasing concentrations of phylloquinone (0, 100, or 500 µM) at 48 hrs. Data represents the results of six different experiments (N = 6).*

The distribution of both annexin V and APO-BrdU non-binding cell area is also unimodal and skewed to the right, with the majority of non-apoptotic cells occupying the left region of the distribution (Figure 18). This distribution indicates a difference between non-apoptotic U937 in the presence of annexin V or APO-BrdU, with those not bound to annexin V generally exhibiting smaller cell areas and those not bound to APO-BrdU exhibiting larger ones. The spread of cell area by assay type,

however, is more consistent, with both annexin V and APO-BrdU cells exhibiting similar ranges in cell area. This data suggests that although there is some difference between cell areas of non-apoptotic U937 in the presence of either annexin V or APO-BrdU, non-apoptotic cell area is less variable than apoptotic area.

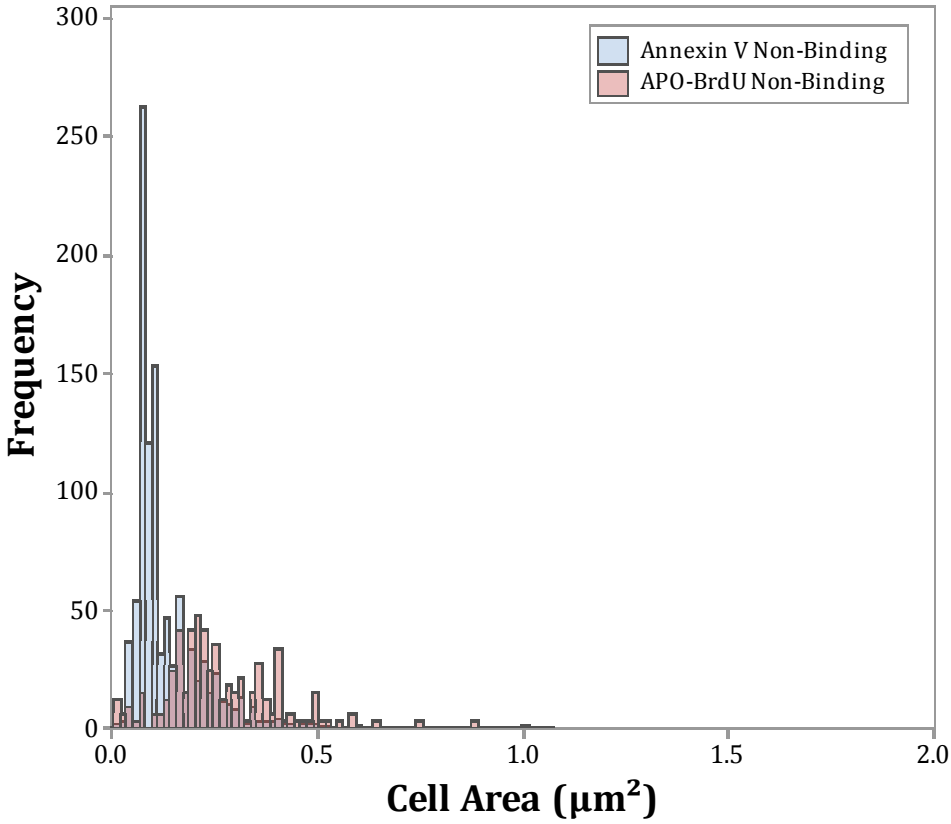

Figure 18: Distribution of Annexin V and APO-BrdU Non-Binding Cell Area Following Treatment with 0, 100, or 500 µM Phylloquinone for 48 Hours. *Distribution of annexin V and APO-BrdU non-binding U937 cell area following treatment with increasing concentrations of phylloquinone (0, 100, or 500 µM) at 48 hrs. Data represents the results of six different experiments (N = 6).*

The distribution of all assayed cells is also unimodal and skewed to the right, with the majority of all apoptotic and non-apoptotic U937 cell areas occupying the left side of the distribution (Figure 19). Apoptotic and non-apoptotic cells are

represented by their binding or non-binding of annexin V or APO-BrdU. The distribution of all assayed cells is consistent with the distribution of overall cell area and is comprised of areas ranging from 0.02 to 1.90 μm^2. The areas of cells binding annexin V appear to be generally smaller than cells not binding annexin V, while areas of cells binding APO-BrdU appear to be generally larger than cells not binding APO-BrdU. In other words, early-stage apoptotic U937 cells exhibit smaller areas than non-apoptotic ones, while late-stage apoptotic U937 cells have larger areas than non-apoptotic ones. In addition, cells binding APO-BrdU appear to have the greatest spread, indicating the areas of late-stage apoptotic U937 are the most variable.

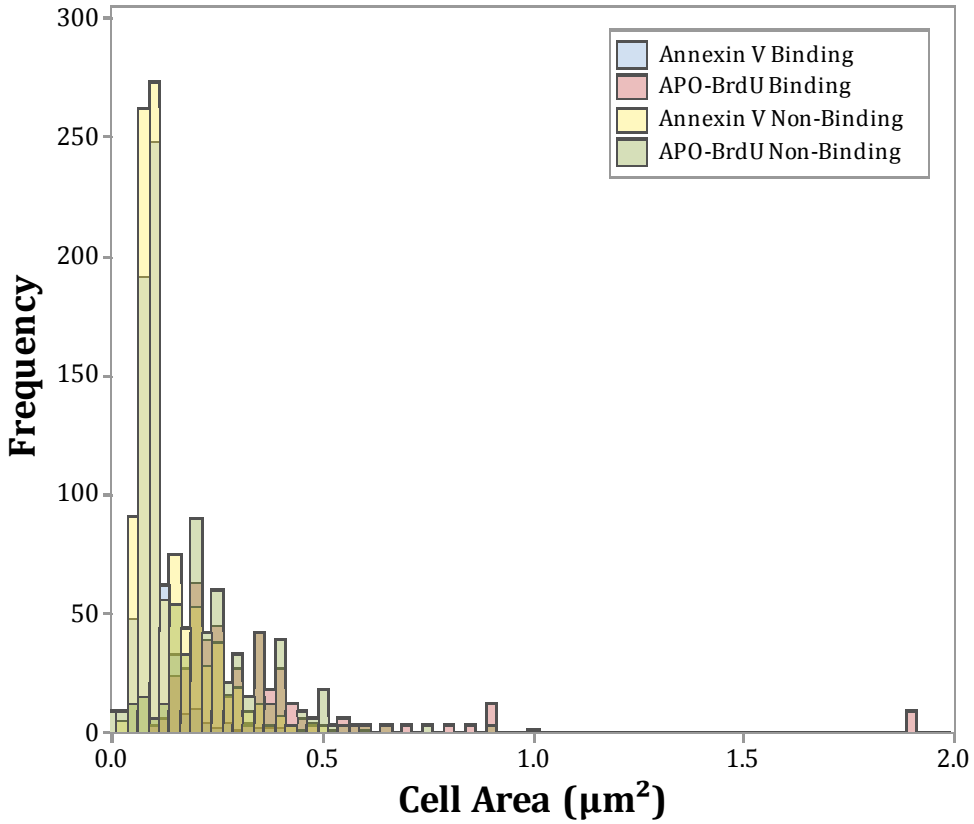

Figure 19: Distribution of Annexin V and APO-BrdU Binding and Non-Binding Cell Area Following Treatment with 0, 100, or 500 µM Phylloquinone for 48 Hours. *Distribution of annexin V and APO-BrdU binding and non-binding U937 cell area following treatment with increasing concentrations of phylloquinone (0, 100, or 500 µM) at 48 hrs. Data represents the results of six different experiments (N = 6).*

Cell Density

U937 cell densities were determined following various concentrations and experimental durations, consisting of 0, 10, 50, 100, and 500 µM phylloquinone and 24 hours to 7 days, depending on the particular experiment (Table 1). Cell densities analyzed by phylloquinone concentration were divided into groups based on experimental duration, which consist of 48 hours (Figure 20) or 7 days (Figures 21 and 22), in addition to 96 hour time course experiments (Figures 23-26). Initial cell

densities were also measured, in order to ensure plating homogeneity (Figure 27). Mean cell density following treatment with 0, 100, or 500 μM phylloquinone for 48 hours exhibits a concentration-dependent reduction in cell density, so that cells treated with 500 μM phylloquinone contain the least amount of viable cells, while cell treated with 0 μM phylloquinone contain the most (Figure 20). Mean cell densities are approximately: 297,000 cells/ml for 0 μM phylloquinone, 211,000 cells/ml for 100 μM phylloquinone, and 117,000 cells/ml for 500 μM phylloquinone. This data was collected from twelve experimental replicates, with initial cell densities of 200,000 cells per ml of suspension. A one-way ANOVA was used to analyze mean cell density following treatment with 100 or 500 μM phylloquinone at 48 hours. The results of this analysis indicate there are significantly different densities between control and treatment groups at 48 hours of treatment, as well as that increasing concentrations of phylloquinone further inhibit U937 cell growth ($F(2, 141) = 48.086$, $p < 0.001$).

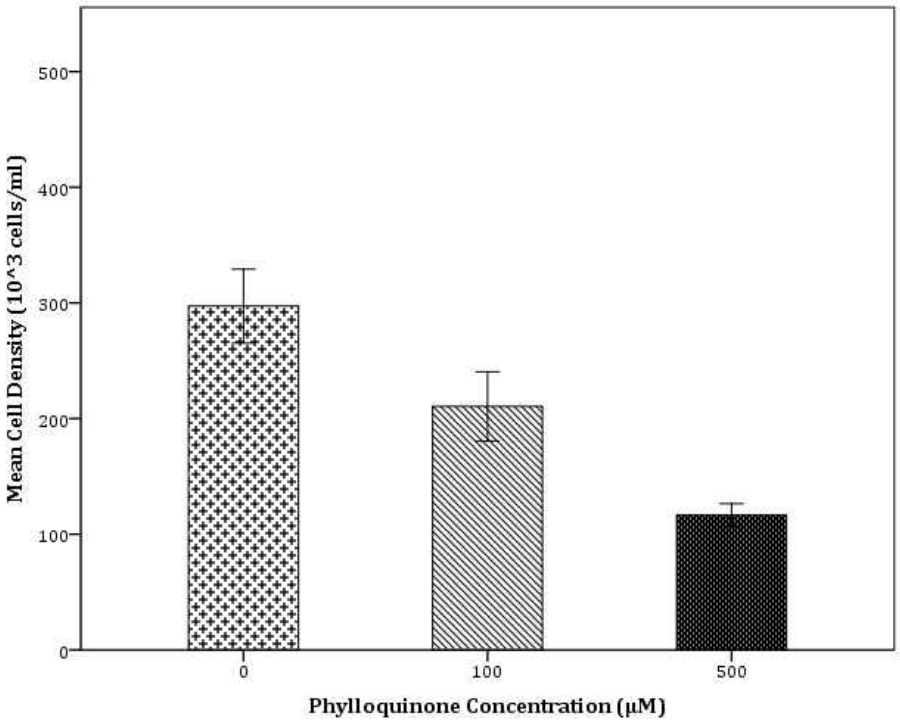

Figure 20: Mean Cell Density Following Treatment with 0, 100, or 500 µM Phylloquinone for 48 Hours. *Mean density of U937 cells following treatment with increasing concentrations of phylloquinone (0, 100 or 500 µM) at 48 hrs. Data represents the results of twelve different experiments (N = 12) (mean ± SEM). Data were analyzed by a one-way ANOVA (F (2, 141) = 48.086, p < 0.001).*

Mean cell density following treatment with 0, 10, 50, 100, or 500 µM phylloquinone at 7 days also exhibits a concentration-dependent reduction in U937 cell numbers, with the highest amount of remaining viable cells in the control group and the least amount remaining in the higher treatment concentration groups (100 or 500 µM phylloquinone) (Figure 21). Mean cell densities for each treatment group are approximately: 305,000 cells/ml for 0 µM phylloquinone, 196,000 cells/ml for 10 µM phylloquinone, 140,000 cells/ml for 50 µM phylloquinone, 94,000 cells/ml for 100 µM phylloquinone, and 95,000 cells/ml for 500 µM phylloquinone. These results vary from the 48 hour density analysis, in that the highest treatment

concentrations yielded cell densities that were close to one another, with a slightly higher reduction of U937 cells treated with 100 μM phylloquinone. This data represents the results of three experimental replicates with initial cell densities of 200,000 cells/ml. A one-way ANOVA was used to analyze mean cell density following treatment with 100 or 500 μM phylloquinone at 7 days. The results of this analysis suggest mean cell densities vary significantly between treatment groups at 7 days of treatment through a concentration-dependent inhibition of cell growth ($F(4, 57) = 4.417$, $p < 0.005$).

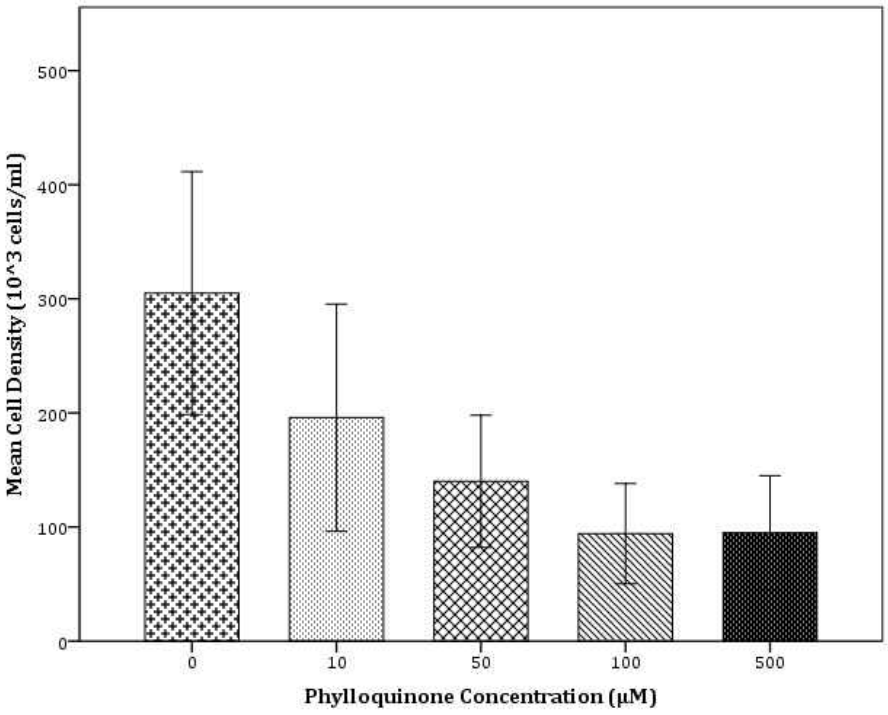

Figure 21: Mean Cell Density Following Treatment with 0, 10, 50, 100, or 500 μM Phylloquinone for 7 days. *Mean density of U937 cells following treatment with increasing concentrations of phylloquinone (0, 10, 50, 100 or 500 μM) at 7 days. Data represents the results of three different experiments (N = 3) (mean ±*

One replicate of this 7 day study was presented as a separate figure due to its variability from other experimental results (Figure 22). A one-way ANOVA was used to analyze this experiment. The results of this analysis indicate cell densities are significantly different between treatment groups, although the relationship between phylloquinone concentration and cell density varies considerably from other experimental replicates ($F(4, 17) = 4.218$, $p < 0.005$).

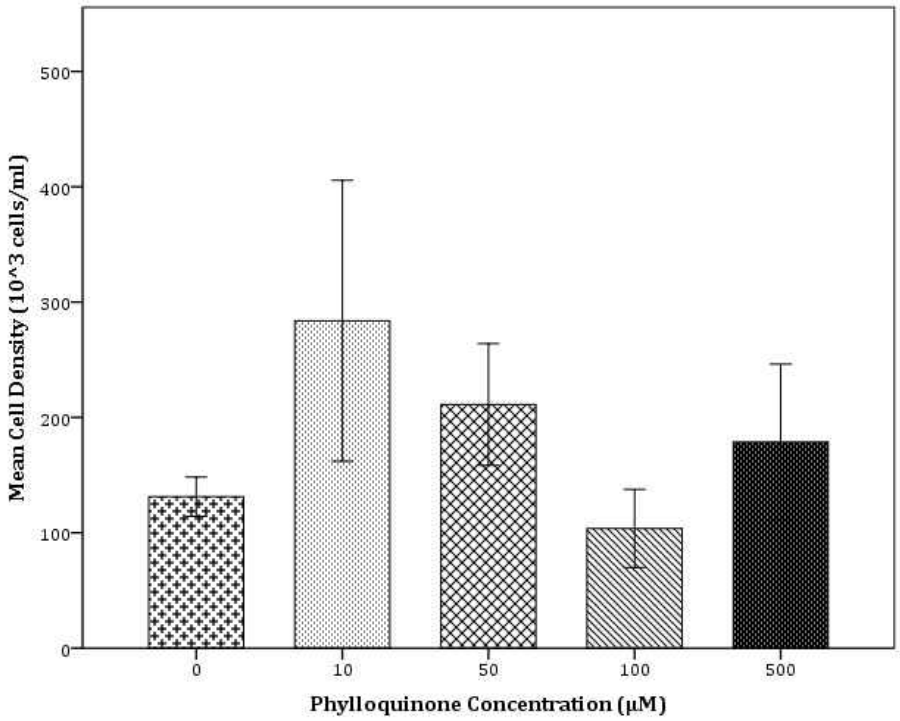

Figure 22: Abnormal Mean Cell Density Following Treatment with 0, 10, 50, 100, or 500 µM Phylloquinone for 7 days. *Mean density of U937 cells following treatment with increasing concentrations of phylloquinone (0, 10, 50, 100 or 500 µM) at 7 days. Data represents the results of one experiment (N = 1) (mean ± SEM). Data was analyzed by a one-way ANOVA (F (4, 17) = 4.218, p < 0.005).*

Time course experiments consisted of treatment with 0, 100, or 500 µM phylloquinone for 96 hours, with cell counts conducted every 24 hours. These

experiments exhibited both a concentration- and time-dependent reduction in viable U937 cells treated with 100 or 500 μM phylloquinone, while untreated U937 cells density increased over time (Figure 23). Following 24 hours of treatment, cells cultured in 0 μM phylloquinone have the highest mean density, while cells treated with 500 μM have the lowest. This relationship is maintained and enhanced over time, so that at 96 hours of treatment, U937 cells treated with no phylloquinone have densities that are higher than both other treatment concentrations (100 μM or 500 μM), as well as higher for the same group on previous days (24, 48, and 72 hours). The treated groups exhibit the inverse of this trend, with the largest reduction of U937 cell densities in groups treated with 500 μM phylloquinone for 96 hours, when compared to other concentrations of phylloquinone (0 or 100 μM) and other days (24, 48, and 72 hours). This data represents the results of three experimental replicates with initial densities of 100,000 cells/ml. A two-way ANOVA was conducted on cell densities following treatment with 100 or 500 μM at 24, 48, 72, and 96 hours. The results of this analysis suggest mean cell area is significantly different between treatment concentrations and over time, and that phylloquinone is able to exert both a concentration- and time-dependent inhibition of U937 cell growth ($F(6, 141) = 6.759$, $p < 0.001$). The two-way ANOVA was also used to generate two line graphs depicting estimated marginal means of cell density over time or by phylloquinone concentration, which again depict its concentration and time-dependent effects (Figures 24 and 25).

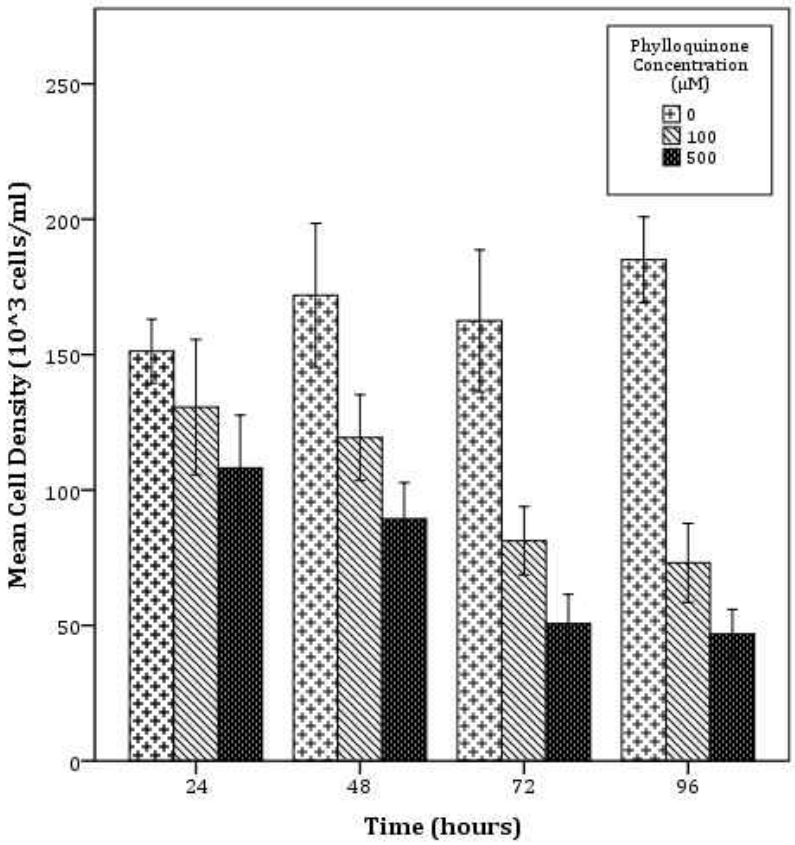

Figure 23: Mean Cell Density Following Treatment with 0, 100, or 500 µM Phylloquinone for 24, 48, 72, or 96 Hours. *Mean density of U937 cells following treatment with increasing concentrations of phylloquinone (0, 100 or 500 µM) at 24, 48, 72, or 96 hrs. Data represents the results of three different experiments (N = 3) (mean ± SEM). Data was analyzed by a two-way ANOVA (F (6, 141) = 6.759, p < 0.001).*

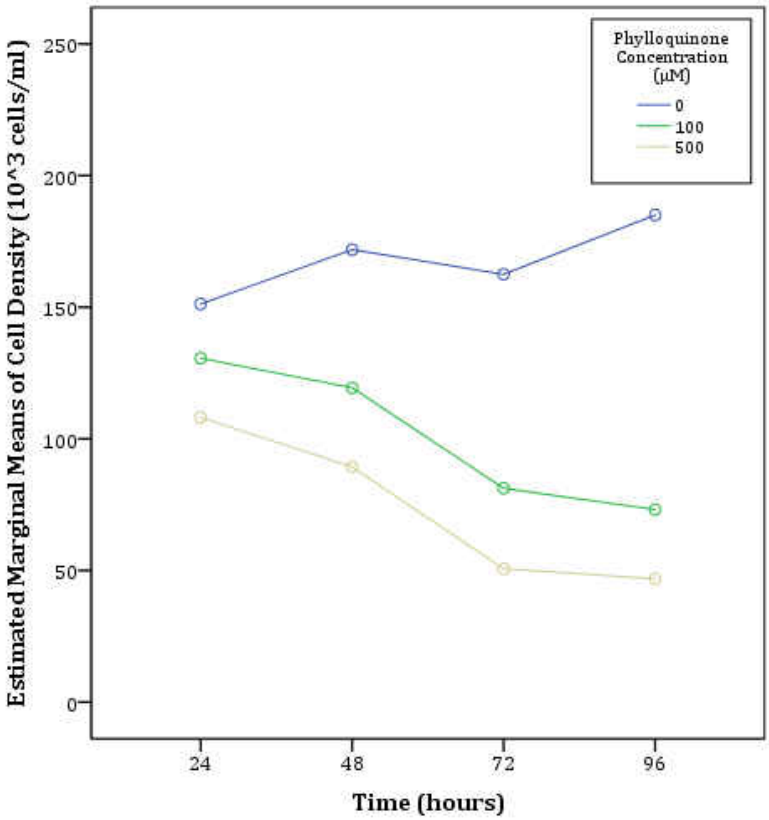

Figure 24: Estimated Marginal Means of Cell Density Following Treatment with 0, 100, or 500 µM Phylloquinone Over Time (24, 48, 72, or 96 Hours). *Estimated marginal means of U937 cell density following treatment with increasing concentrations of phylloquinone (0, 100 or 500 µM) over time (24, 48, 72, or 96 hrs). Data represents the results of three different experiments (N = 3).*

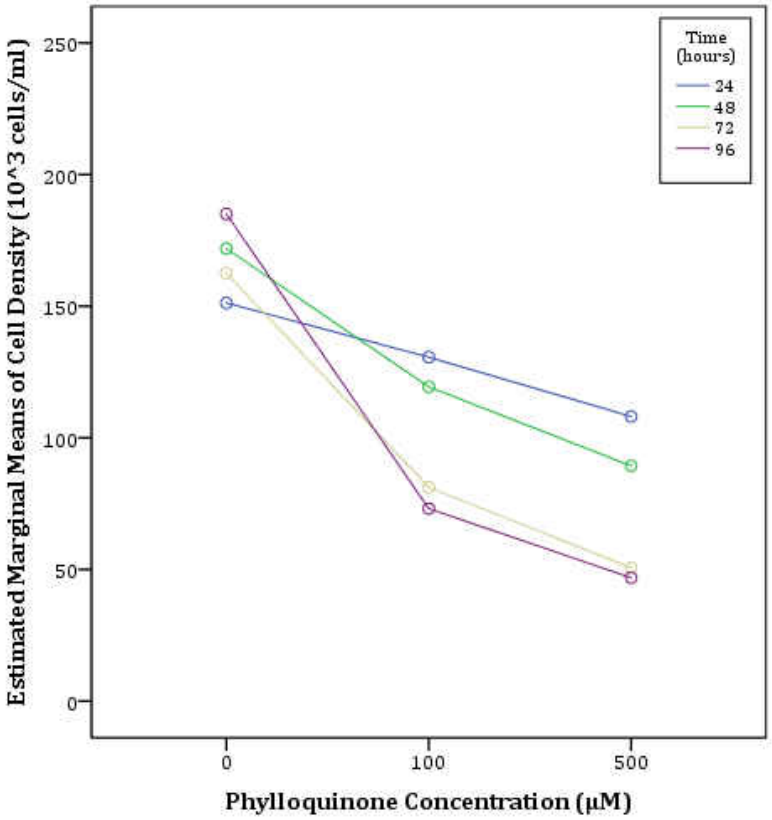

Figure 25: Estimated Marginal Means of Cell Density By Phylloquinone Treatment Concentration (0, 100, or 500 µM) for 24, 48, 72, or 96 Hours. *Estimated marginal means of U937 cell density by phylloquinone treatment concentration (0, 100 or 500 µM) for 24, 48, 72, or 96 hrs. Data represents the results of three different experiments (N = 3).*

U937 cell densities were also examined prior to treatment with phylloquinone to ensure both sample and replicate homogeneity, and were analyzed for 0, 100, or 500 µM phylloquinone (Figure 26). This data represents the results of four experimental replicates, where initial cell densities were projected at 200,000 cells/ml. It appears that each sample had a mean initial density of slightly over this amount (approximately 231,000 cells/ml for 0 µM phylloquinone, 234,000 cells/ml for 100 µM phylloquinone, and 230,000 cells/ml for 500 µM phylloquinone). A one-way ANOVA was conducted on mean cell density prior to treatment with

phylloquinone. The results of this analysis show initial cell density does not significantly vary between control and treatment groups, as well as shows that cells were sufficiently homogenized before plating (F (2, 21) = 0.031, p = 0.97).

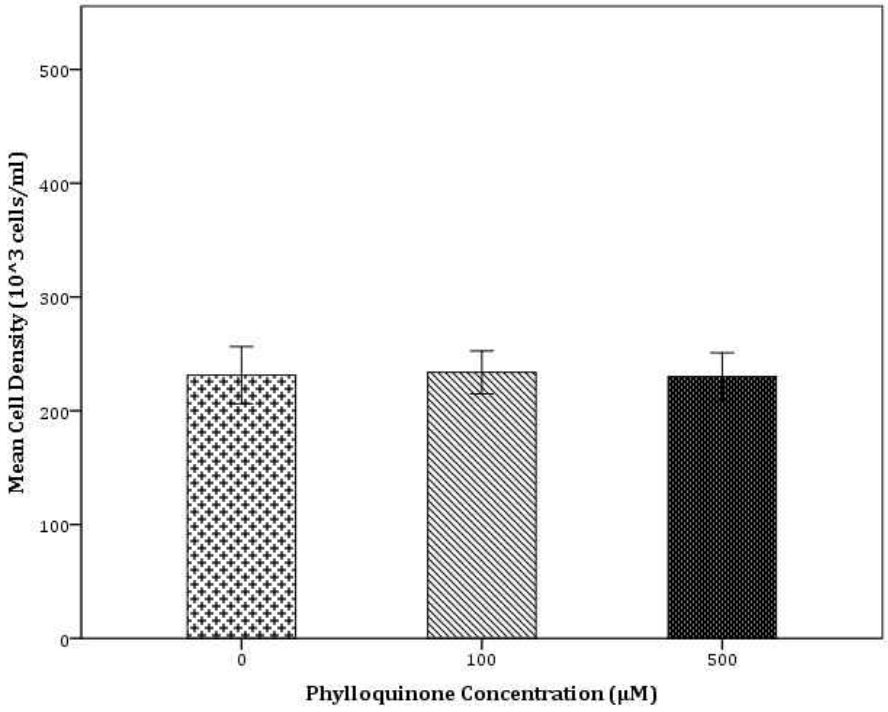

Figure 26: Mean Cell Density Prior to Treatment with 0, 100, or 500 µM Phylloquinone for 48 Hours. *Mean initial U937 cell density prior to treatment with increasing concentrations of phylloquinone (0, 100 or 500 µM) at 48 hrs. Data represents the results of four different experiments (N = 4) (mean ± SEM). Data were analyzed by a one-way ANOVA (F (2, 21) = 0.031, p = 0.97).*

CHAPTER 4

DISCUSSION

The Frequency of Apoptosis is Significantly Higher in U937 Cell Populations, Following Treatment with Phylloquinone

Percent apoptosis data indicate treatment of U937 cells with phylloquinone results in the induction of apoptosis, as well as higher concentrations of phylloquinone increase the frequency of apoptosis. Approximately 10% of untreated U937 cells underwent apoptosis, while 50% of cells treated with 100 μM phylloquinone and 60% of cells treated with 500 μM underwent apoptosis (Table 3). Although there is a concentration-dependent increase in percent apoptosis, there is only about a 10% increase in apoptosis following a fivefold increase in the concentration of phylloquinone. This could be caused by a number of factors including receptor saturation, desensitization, or activation of a different apoptotic pathway. The results of these experiments validate the role of phylloquinone in the induction of apoptosis.

Apoptotic and Non-Apoptotic U937 Cell Areas are Larger Following Treatment with Increasing Concentrations of Phylloquinone

Cell area data and analyses demonstrate treatment with phylloquinone results in U937 cells with considerably larger areas, regardless if the cell is apoptotic or not (Figures 7 – 16). In addition, this effect is concentration-dependent, so that increasing concentrations of phylloquinone result in increasing cell areas.

This data supports the preliminary data and is believed to be due, in part, to the increased occurrence of apoptosis in treated cell populations (Blair and Miller 2012). The effect of increased area in non-apoptotic U937 cells treated with phylloquinone could also be due to phylloquinone's ability to regulate cell size independently of cell death or because these cells were bound for death but did not emit the signals indicative of early or late-stage apoptosis (i.e. annexin V or APO-BrdU). The results of these experiments show that phylloquinone treatment increases cell size, regardless of the status of cell death.

Early-Stage Apoptotic Cells are Smaller than Late-Stage Apoptotic Cells

Cell area data and analyses demonstrate early-stage apoptotic cells (annexin V binding) have areas that are smaller than non-apoptotic cells (annexin V non-binding), while late-stage apoptotic cells (APO-BrdU binding) have areas that are larger than non-apoptotic cells (APO-BrdU non-binding) (Figures 9 – 19). This data supports preliminary data in that it provides evidence that apoptotic cells are ultimately larger than non-apoptotic ones (Blair and Miller 2012). This change in cell area was originally believed to be due to membrane blebbing, however, this event occurs earlier in apoptosis, and these changes in area do not seem to appear until late-stage apoptosis. This increase in cell area is therefore believed to be due to the formation of apoptotic bodies that occurs during the latter part of apoptosis, and/or to other cellular mechanisms that could have been employed to increase the area of apoptotic cells, such as macrophage differentiation. It is important to note that although cells not binding annexin V or APO-BrdU have areas that increase with

increasing concentrations of phylloquinone, there is a significant difference between the mean area and distributions of these non-apoptotic cells. There are a number of explanations for this difference, including changes that may have occurred to U937 cells during fixation (APO-BrdU™ TUNEL Assay), cells that were undergoing apoptosis did not produce the signals necessary to be classified as apoptotic and were therefore considered non-apoptotic, or again, to other cellular mechanisms that may have been inducted following treatment with phylloquinone (Zhao et al. 2014). Regardless of the reason, the relationship between early and late-stage apoptosis is unaffected, meaning that early-stage apoptotic cells are smaller than late-stage ones.

Phylloquinone Inhibits U937 Cell Growth and These Effects are Enhanced Over Time

Cell density data and analyses indicate treatment with phylloquinone reduces U937 cell growth, and that phylloquinone exerts its effects in a manner that is both concentration- and time-dependent (Figures 20, 21, and 23 – 25). In other words, treatment with higher concentrations of phylloquinone further reduces U937 cell growth, while longer treatment times further enhance this effect. These results are consistent with preliminary data and validate the inhibitory effects of phylloquinone on U937 cell growth (Blair and Miller 2012). One replicate of these experiments produced data that is inconsistent with reduced U937 cell viability following treatment with phylloquinone (Figure 23). This difference in mean cell density is believed to be due to plating heterogeneity or contamination, as data from this replicate is considerably different from other density experiments. The results

of these experiments confirm the inhibitory effect of phylloquinone on U937 cell growth.

CHAPTER 5

CONCLUSION AND FUTURE DIRECTIONS

This study was conducted in order to validate the apoptotic and inhibitory effects of phylloquinone in the U937 cell line. These effects were assessed through the quantification of cell density and area following treatment with phylloquinone, as well as through assay confirmation of the occurrence of apoptosis. The results of this study show that treatment with phylloquinone induces apoptosis, reduces cell growth, and increases cell area, as well as higher concentrations of phylloquinone enhance these effects. These results are significant because they document the chemotherapeutic and cytotoxic potential of this analog of vitamin K in a carcinoma cell line, and in doing so, support former studies involving this compound, as well as the need for additional ones (Wei et al. 2010; Wei et al. 2010; Carr et al. 2011; Linsalata et al. 2015; Orlando et al. 2015). The utilization of phylloquinone to induce cell death and reduce cancer cell proliferation could lead to the development of more effective anti-cancer drugs, as well as the discovery of other preexisting drugs whose effects are enhanced in combination with this compound. These results are also significant because they provide support for studies concerning the anti-cancer effects of nutritive and organic compounds, like vitamins, which are appealing because of their lack of damage to healthy tissues, variety of other health benefits, like immune system enhancement, and implication for cancer prevention (Mora et al. 2008). These results also support other findings regarding the changes in cell size that occur during apoptosis, which consist of an initial reduction in cell area

followed by an increase in area, which is assumed to occur as a result of membrane blebbing or budding (Kerr et al. 1972; Majno and Joris 1995).

Future studies interested in the anti-cancer effects of this compound, alone or in combination with other chemotherapeutic agents, can utilize this study when selecting experimental model (i.e. cell type), phylloquinone concentration, and treatment time. Future studies on this compound may also provide further insight into the evasion of cell death and promotion of tumorgenesis and metastasis, and how to intercede this behavior and dysfunction in cancer cells. These research areas are of particular importance to our understanding of cancer development, improved treatments, and improved prevention.

REFERENCES

Abud H E (2004). "Shaping developing tissues by apoptosis." Cell Death and Differentiation **11**: 797-799.

Alberts B, Johnson A, Lewis J, Raff M, Roberts K, Walter P (2002). "Extracellular Control of Cell Division, Cell Growth, and Apoptosis." Molecular Biology of the Cell. 4th edition. New York: Garland Science.

American Cancer Society (2014). "Evolution of cancer treatments: Chemotherapy." http://www.cancer.org/cancer/cancerbasics/thehistoryofcancer/the-history-of-cancer-cancer-treatment-chemo. Visited 4.12.2016.

American Cancer Society (2015). "Cancer Facts & Figures 2015." http://www.cancer.org/acs/groups/content/@editorial/documents/document/acspc-044552.pdf. Visited 4.12.2016.

Ascaso R, Marvel J, Collins MK, López-Rivas A (1994). "Interleukin-3 and Bcl-2 cooperatively inhibit etoposide-induced apoptosis in a murine pre-B cell line." European Journal of Immunology **24**(3): 537-541.

Blair T, Miller H (2012). "Effect of Vitamin K1 on Cell Growth Inhibition and Apoptosis on the U937 Cell Line." Journal of Cancer Therapy **3**(2): 167-172.

Bold R J, Termuhlen P M, McConkey D J (1997). "Apoptosis, cancer, and cancer therapy." Surgical Oncology **6**(3): 133-142.

Carr B I, Wang Z, Wang M, Cavallini A, D'Alessandro R, Refolo M G (2011). "c-Met-Akt pathway-mediated enhancement of inhibitory c-Raf phosphorylation is involved in vitamin K1 and sorafenib synergy on HCC growth inhibition." Cancer Biology & Therapy **12**(6): 531-538.

ChemSpider. "Phylloquinone (ChemSpider ID: 4447652)." http://www.chemspider.com/Chemical-Structure.4447652.html. Visited 4.12.2016.

Chang H W, Yang X (2000). "Proteases for Cell Suicide: Functions and Regulation of Caspases." Microbiology and Molecular Biology Reviews **64**(4): 821-846.

Clarke P G H, Clarke S (2012). "Nineteenth Century Research On Cell Death." Experimental Oncology **34** (3).

Council for Responsible Nutrition (2013). "Vitamin and Mineral Safety." 3rd Edition. http://www.crnusa.org/safety/updatedpdfs/09-CRNVMS3-VITAMINK.pdf. Visited 4.12.2016.

Criddle D N, Gillies S, Baumgartner-Wilson H K, Jaffar M, Chinje E C, Passmore S, Chvanov M, Barrow S, Gerasimenko O V, Tepikin A V et al. (2006). "Menadione-induced Reactive Oxygen Species Generation via Redox Cycling Promotes Apoptosis of Murine Pancreatic Acinar Cells." The Journal of Biological Chemistry **281**(52): 40485-40492.

Dorn G W (2013). "Molecular Mechanisms That Differentiate Apoptosis from Programmed Necrosis." Toxicologic Pathology **41**(2): 227-234.

Ehrlich S D (2013). "Vitamin K." University of Maryland Medical Center. http://umm.edu/health/medical/altmed/supplement/vitamin-k. Visited 4.12.2016.

Elliot M R, Ravichandran K S (2010). "Clearance of apoptotic cells: implications in health and disease." The Journal of Cell Biology **189** (7): 1059-1070.

Elmore S (2007). "Apoptosis: A Review of Programmed Cell Death." Toxicologic Pathology **35**(4): 495-516.

Fasth A E R, Snir O, Johansson A T, Nordmark B, Rahbar A, af Klint E, Björkström N K, Ulfgren A, van Vollenhoven R F, Malmström V et al. (2007). "Skewed distribution of proinflammatory $CD4^{+}CD28^{null}$ T cells in rheumatoid arthritis." Arthritis Research & Therapy 9(5): 1-11.

Fieser L F, Tishler M, Sampson W L (1941). "Vitamin K Activity and Structure." The Journal of Biochemistry **137** (2): 559-692.

Hazell S (2014). "Mustard gas – from the Great War to frontline chemotherapy." http://scienceblog.cancerresearchuk.org/2014/08/27/mustard-gas-from-the-great-war-to-frontline-chemotherapy/. Visited 4.12.2016.

Higdon J (2000). "Vitamin K." Linus Pauling Institute – Oregon State University. http://lpi.oregonstate.edu/mic/vitamins/vitamin-K. Visited 4.12.2016.

Hinshaw V S, Olsen C W, Dybdahl-Sissoko N, Evans D (1994). "Apoptosis: a mechanism of cell killing by influenza A and B viruses." Journal of Virology **68** (6): 3667-3673.

Hitomi M, Yokoyama F, Kita Y, Nonomura T, Masaki T, Yoshiji H, Inoue H, Kinekawa F, Kurokohchi K, Uchida N et al. (2005). "Antitumor effects of vitamins K1, K2 and K3 on hepatocellular carcinoma in vitro and in vivo." Journal of Oncology **26**(3): 713-720.

Howell A, Anderson A S, Clarke R B, Duffy S W, Evans D G, Garcia-Closas M, Gescher A J, Key T J, Saxton J M, Harvie M N (2014). "Risk determination and prevention of breast cancer." Breast Cancer Research **16**(5): 446–464.

Issaeva N, Przemyslaw B, Enge M, Protopopova M, Verhoef L G C, Masucci M, Pramanik A, Selivanova G (2004). "Small molecule RITA binds to p53, blocks p53-HDM-2 interaction and activates p53 function in tumors." Nature Medicine **10**: 1321-1328.

Jiang L (2011). " "Apoptosis: A Basic Biological Phenomenon with Wide-Ranging Implications in Tissue Kinetics" (1972), by John F. R. Kerr, Andrew H. Wyllie, and Alastair R. Currie." Embryo Project Encyclopedia: ISSN: 1940-5030. http://embryo.asu.edu/handle/10776/2312. Visited 9.6.2015.

Johnstone R W, Frew A J, Smyth M J (2008). "The TRAIL apoptotic pathway in cancer onset, progression and therapy." Nature Reviews Cancer **8**: 782-798.

Johnstone R W, Ruefli A, Lowe S W (2002). "Apoptosis: A Link between Cancer Genetics and Chemotherapy." Cell **108**(2): 153-164.

Karasawa S, Azuma M, Kasama T, Sakamoto S, Kabe Y, Imai T, Yamaguchi Y, Miyazawa K, Handa H (2013). "Vitamin K2 Covalently Binds to Bak and Induces Bak-Mediated Apoptosis." Molecular Pharmacology **83**(3): 613-620.

Kerr J F R (1971). "Shrinkage Necrosis: A Distinct Mode of Cellular Death." Journal of Pathology **105**(1): 13–20.

Kerr J F R (2002): "History of the events leading to the formulation of the apoptosis concept." Toxicology **181–182**: 471–474.

Kerr J F R, Harmon B, Searle J (1974). "An electron-microscope study of cell deletion in the anuran tadpole tail during spontaneous metamorphosis with special reference to apoptosis of striated muscle fibres." Journal of Cell Science **14**: 571-585.

Kerr J F R, Winterford C M, Harmon B V (1994): "Apoptosis: Its Significance in Cancer and Cancer Therapy." Cancer **73**(8): 2013-2025.

Kerr J F R, Wyllie A H, Currie A R (1972). "Apoptosis: A Basic Biological Phenomenon with Wide-ranging Implications in Tissue Kinetics." British Journal of Cancer **26**(4): 239-257.

Kholoussi N M, El-Nabi S E H, Esmaiel N, El-Bary N M A, El-Kased A F (2014). "Evaluation of Bax and Bak Gene Mutations and Expression in Breast Cancer." BioMed Research International **2014**: 1-9.

Linsalata M, Orlando A, Tutino V, Notarnicola M, D'Attoma B, Russo F (2015). "Inhibitory effect of vitamin K1 on growth and polyamine biosynthesis of human gastric and colon carcinoma cell lines." Journal of Oncology **47**(2): 773-781.

Lockshin R A, Zakeri Z (2001). "Programmed cell death and apoptosis: origins of the theory." Nature Reviews Molecular Cell Biology **2**(7): 545-550.

Lowe S, Lin A (2000). "Apoptosis in cancer." Carcinogenesis **21**(3): 485-495.

Majno G, Joris I (1995): "Apoptosis, Oncosis, and Necrosis: An Overview of Cell Death." American Journal of Pathology **146**(1): 3–15.

Markel H (2015). "How playing with dangerous x-rays led to the discovery of radiation treatment for cancer." http://www.pbs.org/newshour/updates/emil-grubbe-first-use-radiation-treat-breast-cancer/. Visited 4.12.2016.

Marks J (1975). "The Fat-Soluble Vitamins in Modern Medicine." Vitamins & Hormones **32**: 131-154.

Martin S J, Green D R (1995): "Apoptosis and cancer: the failure of controls on cell death and cell survival." Critical Reviews in Oncology/Hematology **18**: 137-153.

Mathiasen I S, Lademann U, and Jäättelä M (1999). "Apoptosis Induced by Vitamin D Compounds in Breast Cancer Cells Is by Bcl-2 but Does Not Involve Known Caspases or p53." Cancer Research **59**: 4848-4856.

McCubrey J A, Steelman L S, Chappell W H, Abrams S L, Wong E W T, Chang F, Lehmann B, Terrian D M, Milella M, Tafuri A et al. (2007). "Roles of the RAF/MEK/ERK Pathway in Cell Growth, Malignant Transformation and Drug Resistance." Biochimica et Biophysica Acta – Molecular Cell Research **1773**(8): 1263-1284.

Mora J R, Iwata M, von Andrian U H (2008). Vitamin effects on the immune system: vitamins A and D take centre stage." Nature Reviews Immunology **8**(9): 685-698.

National Cancer Institute (2014). "Targeted Cancer Therapies." http://www.cancer.gov/about-cancer/treatment/types/targeted-therapies/targeted-therapies-fact-sheet. Visited 4.12.2016.

National Cancer Institute (2015). "Types of Treatment." http://www.cancer.gov/about-cancer/treatment/types. Visited 4.12.2016.

National Cancer Institute (2015). "Global Health and Cancer Epidemiology." http://epi.grants.cancer.gov/global-health/. Visited 4.12.2016.

National Center for Biotechnology Information. (2015). PubChem Compound Database. "Menadione."

https://pubchem.ncbi.nlm.nih.gov/compound/4055#section=Top. Visited 11.23.2015.

National Center for Biotechnology Information. (2015). PubChem Compound Database. "Menaquinone-2." https://pubchem.ncbi.nlm.nih.gov/compound/5280374#section=Top. Visited 11.23.2015.

National Center for Biotechnology Information. (2015). PubChem Compound Database. "Phylloquinone." https://pubchem.ncbi.nlm.nih.gov/compound/4812#section=Top. Visited 11.23.2015.

National Institute of Health (2016). "Estimates of Funding for Various Research, Condition, and Disease Categories (RCDC)." https://report.nih.gov/categorical_spending.aspx. Visited 2.25.2016.

National Institute of Health (2015). "Vitamin K." https://ods.od.nih.gov/factsheets/VitaminK-HealthProfessional/. Visited 4.12.2016.

Orlando A, Linsalata M, Tutino V, D'Attoma B, Notarnicola M, Russo F (2015). "Vitamin K1 Exerts Antiproliferative Effects and Induces Apoptosis in Three Differently Graded Human Colon Cancer Cell Lines." BioMed Research International **2015**: 1-15.

Ouyang H, Furukawa T, Abe T, Kato Y, Horii A (1998). "The BAX gene, the promoter of apoptosis, is mutated in genetically unstable cancers of the colorectum, stomach, and endometrium." Clinical Cancer Research **4**: 1071-1074.

Panayi N D, Mendoza E, Breshears E S, Burd R (2013). "Aberrant Death Pathways in Melanoma." Recent Advances in the Biology, Therapy, and Management of Melanoma. http://www.intechopen.com/books/recent-advances-in-the-biology-therapy-and-management-of-melanoma/aberrant-death-pathways-in-melanoma. Visited 4.12.2016.

Passmore J S, Lukey P T, Ress S R (2001). "The human macrophage cell line U937 as an *in vitro* model for selective evaluation of mycobacterial antigen-specific cytotoxic T-cell function." Immunology **102**(2): 146-156.

Peterson E, Prithwish D, Nuttall R (2012). "BMI, Diet and Female Reproductive Factors as Risks for Thyroid Cancer: A Systematic Review." PLoS One **7**(1): e29177.

Rodríguez-Grille J, Busch L K, Martínez-Costas J, Benavente J (2014). "Avian reovirus-triggered apoptosis enhances both virus spread and the processing of the viral nonstructural muNS protein. Virology **462-463**: 49-59.

Sak K (2012). "Chemotherapy and Dietary Phytochemical Agents." Chemotherapy Research and Practice **2012**: 1-11.

Sakagami H, Satoh K, Hakeda Y, Kumegawa M (2000). "Apoptosis-inducing activity of vitamin C and vitamin K." Cellular and Molecular Biology **46**(1): 129-143.

Sigma Aldrich (2015). "U937 Cell Line human." Sigma-Aldrich. http://www.sigmaaldrich.com/catalog/product/sigma/85011440?lang=en&region=US. Visited 11.23.2015.

Silva M T (2010): "Secondary necrosis: The natural outcome of the complete apoptotic program." FEBS Letters **584**(22): 4491-4499.

Solary E, Dubrez L, Eymin B (1996). "The role of apoptosis in the pathogenesis and treatment of diseases." European Respiratory Journal **9**: 1293-1305.

Sudhakar A (2009). "History of Cancer, Ancient and Modern Treatment Methods." Journal of Cancer Science & Therapy **1** (2): 1-4.

Sundström C, Nilsson K (1976). "Establishment and characterization of a human histiocytic lymphoma cell line (U-937)." International Journal of Cancer **17** (5): 565-577.

Suresh S, Raghu D, Karunagaran D (2013). "Menadione (Vitamin K3) induces apoptosis of human oral cancer cells and reduces their metastatic potential by modulating the expression of epithelial to mesenchymal transition markers and inhibiting migration." Asian Pacific Journal of Cancer Prevention **14**(9): 5461-5465.

Sylvester P W (2007). "Vitamin E and apoptosis." Vitamins and Hormones **76**: 329-356.

ThermoFisher Scientific (2015). "APO-BrdU™ TUNEL Assay Kit, with Alexa Fluor® 488 Anti-BrdU." ThermoFisher Scientific. https://www.thermofisher.com/order/catalog/product/A23210. Visited 11.24.2015.

Tsujioka T, Miura Y, Otsuki T, Nishimura Y, Hyodoh F, Wada H, Sugihara T (2006). "The mechanisms of vitamin K2-induced apoptosis of myeloma cells." Haematologica **91**(5): 613-619.

Turk B, Stoka V (2007). "Protease signaling in cell death: caspases versus cysteine cathepsins." FEBS Letters **581**(15): 2761-2767.

van Engeland M, Nieland L J W, Ramaekers F C S, Schutte B, and Reutelingsperger C P M (1998). "Annexin V-Affinity Assay: A Review on an Apoptosis Detection System Based on Phosphatidylserine Exposure." **31**(1): 1-9.

Wang S, El-Deiry W S (2003). "TRAIL and apoptosis induction by TNF-family death receptors." Oncogene **22**: 8628-8633.

Wang Z, Sun Y (2010). "Targeting p53 for Novel Anticancer Therapy." Translational Oncology **3**(1): 1-12.

Wei G, Wang M, Carr B I (2010). "Sorafenib combined vitamin K induces apoptosis in human pancreatic cancer cell lines through RAF/MEK/ERK and c-Jun NH2-terminal kinase pathways." Journal of Cellular Physiology **224**(1): 112-119.

Wei G, Wang M, Hyslop T, Wang Z, Carr B I (2010). "Vitamin K enhancement of Sorafenib-mediated HCC cell growth inhibition *in vitro* and *in vivo*." International Journal of Cancer **127**: 2949-2958.

Williams G T, Smith C A (1993). "Molecular regulation of apoptosis: genetic controls on cell death." Cell **74**(5): 777-779.

Yaguchi M, Miyazawa K, Katagiri T, Nishimaki J, Kizaki M, Tohyama K, Toyama K (1997). "Vitamin K2 and its derivatives induce apoptosis in leukemia cells and enhance the effect of all-trans retinoic acid." Leukemia **11**(6): 779-787.

Yoshida T, Miyazawa K, Kasuga I, Yokoyama T, Minemura K, Ustumi K, Aoshima M, Ohyashiki K (2003). "Apoptosis induction of vitamin K2 in lung carcinoma cell lines: the possibility of vitamin K2 therapy for lung cancer." International Journal of Oncology **23**(3): 627-632.

Yip K W, Reed J C (2008). “Bcl-2 family proteins and cancer.” Oncogene **27**: 6398-6406.

Zhang T, Lu H, Shang X, Tian Y, Zheng C, Wang S, Cheng H, Zhou R (2006). “Nicotine prevents the apoptosis induced by menadione in human lung cancer cells.” Biochemical and Biophysical Research Communications **342**(3): 928-934.

Zhang Y, Zhang B, Zhang A, Zhao Y, Zhao J, Liu J, Gao J, Fang D, Rao Z (2012). “Synergistic growth inhibition by sorafenib and vitamin K2 in human hepatocellular carcinoma cells.” Clinics **67**(9): 1093-1099.

Zhao S, Liao H, Ao M, Wu L, Zhang X, Chen Y (2014). “Fixation-induced cell blebbing on spread cells inversely correlates with phosphatidylinositol 4,5-biphosphate level in the plasma membrane.” FEBS Open Bio **4**: 190-199.

VITA

TESHA BLAIR

Education:	M.S. Biology, East Tennessee State University, Johnson City, Tennessee 2016 B.S. Biology, East Tennessee State University, Johnson City, Tennessee, 2013
Professional Experience:	Research Assistant, East Tennessee State University, Quillen College of Medicine, Department of Biomedical Sciences, 2015-2016 Graduate Assistant, East Tennessee State University, College of Arts and Sciences, 2013-2015
Publications:	Blair T, Miller H (2012). "Effect of Vitamin K1 on Cell Growth Inhibition and Apoptosis on the U937 Cell Line." Journal of Cancer Therapy **3**(2): 167-172
Honors and Awards:	1st Place Poster Presentation, Appalachian Student Research Forum, Natural Sciences Division, 2015 Student-Faculty Collaborative Grant Recipient ($1200), 2011